

FRI-UW-8126  
December 1981

FISHERIES RESEARCH INSTITUTE  
School of Fisheries  
University of Washington  
Seattle, Washington 98195

MEASUREMENTS OF ACOUSTIC BACKSCATTERING DIRECTIVITY  
AND TARGET STRENGTH OF SALMONIDS

by

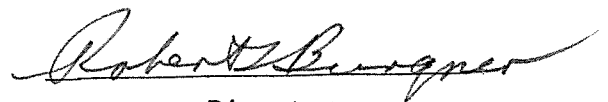
Peter H. Dahl and Ole A. Mathisen

FINAL REPORT

for the period 5/1/81-10/31/81  
Washington State Department of Fisheries

Submitted December 9, 1981

Approved



Director

## INTRODUCTION

Salmon harvest management relies on accurate estimates of escapement to secure adequate spawning populations. The systematic development of echosounders to estimate salmon escapement is motivated by the possibility of increased sampling power and tighter bounds on abundance estimates, ability to provide estimates in glaciated streams where water turbidity prevents visual counting, as well as increased consistency and reliability. Echosounders can be deployed in remote locations upstream, where harvesting has stopped and escapement is complete. Application of echosounders in Alaskan rivers is reviewed by Menin and Paulis (1975) and Davis (1972).

Problems with using echosounders in the riverine environment, such as high ambient noise and false detection, have been identified and are now being addressed with improved signal processing techniques. New Doppler-based signal processing (Carlson and Acker 1979-1980) is directed toward the problem of high density runs such as in Bristol Bay. Lacking in the data base is information on salmonid target strength, which is a measure of the acoustic size of the fish. Instead, literature values obtained from non-salmonid species are used, which can be misleading. Since the axis of the ascending fish generally is parallel to the riverbank and athwart to the transducer, target strength of the side aspect becomes a crucial parameter.

This report summarizes the findings of a contract with the Washington State Department of Fisheries to measure side aspect target strength of salmonids at 420 kHz, the expected operating frequency of a river sonar system. Results include polar plots of fish directivity (target strength variation as fish rotates in yaw or coronal plane), as well as explicit

expressions for target strength probability density and distribution, expected value and variance.

### Target Strength Background

Target strength is the backscattered echo level corrected for fish position in the sonar beam and transmission loss. Target strength (TS) is defined as

$$TS = 10 \log \frac{\delta_{bs}}{4\pi}$$

where  $\delta_{bs}$  is the backscattering cross-section or acoustic size (in meter<sup>2</sup>), and  $4\pi$  is the normalizing constant — the backscattering cross-section of a 2-meter radius reference sphere. Therefore target strength will be the echo level in dB above that of the reference sphere. The definition of target strength as used in this work is that given in Forbes and Nakken (1972).

The backscattering cross-section is related to target surface area, for example it is well established (Nakken and Olsen 1977) that target strength increases with fish length. However, the backscattering cross-section is also dependent upon target physical characteristics and target orientation in the sonar beam, or aspect.

Fish target strength estimates are necessary to obtain quantitative information from hydroacoustic data. For example, fish detection probability is a function of target strength, therefore relative error of fish abundance estimates will depend on the accuracy with which target strength properties are known. Also, with knowledge of expected fish target strength, system source level (SL) can be minimized to avoid excess reverberation which is

especially important in riverine environments. This is evident from the sonar equation expressed in dB (see Urick 1975),

$$EL = TS + SL - 2TL + 2B(\phi, \theta) \quad (1)$$

where  $EL$  = echo level  
 $2TL$  = two-way transmission loss  
 $2B(\phi, \theta)$  = two-way beam pattern gain.

Reflected pressure waves from a fish target are converted to voltage at the sonar's transducer face. The resultant voltage from an echo is proportional to the square root of the target backscattering cross-section,

$$V_{\text{fish}} \sim \sqrt{\delta_{\text{bs}}}$$

where  $V_{\text{fish}}$  is the peak echo envelope voltage from a fish.

Using a reference target with a known target strength, it is convenient to calculate target strength using the expression below which follows from the basic sonar equation

$$TS_{\text{fish}} = 20 \log \frac{V_{\text{fish}}}{V_{\text{ref}}} + TS_{\text{ref}} \quad (2)$$

where  $TS_{\text{fish}}$  = fish target strength  
 $TS_{\text{ref}}$  = reference target strength (known)  
 $V_{\text{ref}}$  = received envelope voltage from reference.

Variance in  $V_{\text{ref}}$  is due to random propagation effects and electronic drift within system hardware. This variance component is negligible when compared

with the variance in  $V_{\text{fish}}$ , and can be ignored in the calculation of fish target strength.

There are theoretical arguments for echo envelope voltage amplitude from an on-axis fish target to be Rayleigh distributed (Clay and Medwin 1977). These arguments follow from the assumption that the structural heterogeneity of the fish body gives rise to a number of discrete sound scattering sources. From the central limit theorem, the resulting scattered pressure level should be Gaussian distributed, which corresponds to a Rayleigh distribution for the echo voltage envelope. Huang and Clay (1980) have examined the statistical properties of target strength in this context; however, no statistical verification of the Rayleigh model was reported. Ehrenberg et al. (1980) have observed a better fit to the Rayleigh model with increasing fish length to wavelength ( $L/\lambda$ ) ratio. Given a typical length of an adult sockeye salmon to be 50 cm, the  $L/\lambda$  ratio at 420 kHz will be about 140. The Rayleigh probability density function is

$$f_Z(z) = \frac{z}{a} e^{-\left(\frac{z^2}{2a}\right)} \quad (3)$$

where

$Z$  = peak detected voltage or equivalently the square root of the back-scattering cross-section

$a$  = the single Rayleigh parameter.

The validity of the Rayleigh assumption will be an important factor for the data analysis and in determining target strength statistics.

## MATERIALS AND METHODS

### Experimental Fish

The fish originated from University of Washington and National Marine Fisheries Service hatchery stocks; two species of salmonids, Salmo gairdneri and Salmo clarki were used. Table 1 in the Results section summarizes data on species, length and weight. The length range of the experimental fish is similar to that found in the catches of sockeye salmon fisheries. Availability and handling tolerance influenced the choice of fish, as the experiment subjected the fish to significant handling stress.

### Study Site

Target strength measurements were made aboard the Applied Physics Laboratory acoustic research barge "R/V. Henderson", moored in the Lake Washington Ship Canal.

### Instrumentation and Data Recording

A Biosonics (Model 101) scientific echosounder was used. The 8 kHz heterodyned output from the sounder was AM recorded on a SONY (Model TC-05M) cassette recorder. The 9° half angle transducer was built by APL; a polar plot of the transducer beam pattern is included in Appendix A.

### Experimental Procedure

A harness constructed from monofilament line was used to position fish for the acoustic measurements. Fish were held within the harness by a small

nylon tie attached to a medical suture anterior to the dorsal fin. The sutures placed in the musculature 3-4 weeks prior to measurements served as multiple-use attachment points for the harness.

Fish were anesthetized with a solution of etomidate (3.0 ppm); at this concentration fish remained tranquilized for approximately 15 min. The anesthetized fish was placed in harness and then lowered two meters below the surface at the acoustic research barge. The transducer, also at depth two meters, was positioned four meters from the fish.

The harness allowed for fixed positioning of the fish or rotation of the fish in the yaw (coronal) plane, while acoustic measurements were made. A diagram of fish within harness is presented in Figure 1. Measurements were made at fixed head aspect, 45° off head aspect and side aspect, with 0.4 msec pulse length. Polar plots were made under continuous rotation measurements. The fish were held within 1 dB of the unity gain portion of sonar beam at all times.

#### Data Processing

Two independent methods were used to process the acoustic data and obtain target strength output. Polar plots of fish target strength vs. orientation angle or aspect were produced during the experiment. Signal processing hardware on the acoustic barge automatically calculates target strength from received voltage and measured system parameters as per the sonar equation, and plots target strength as a function of time on a rotating axis.

In addition, data were recorded at the site in analog form on cassette

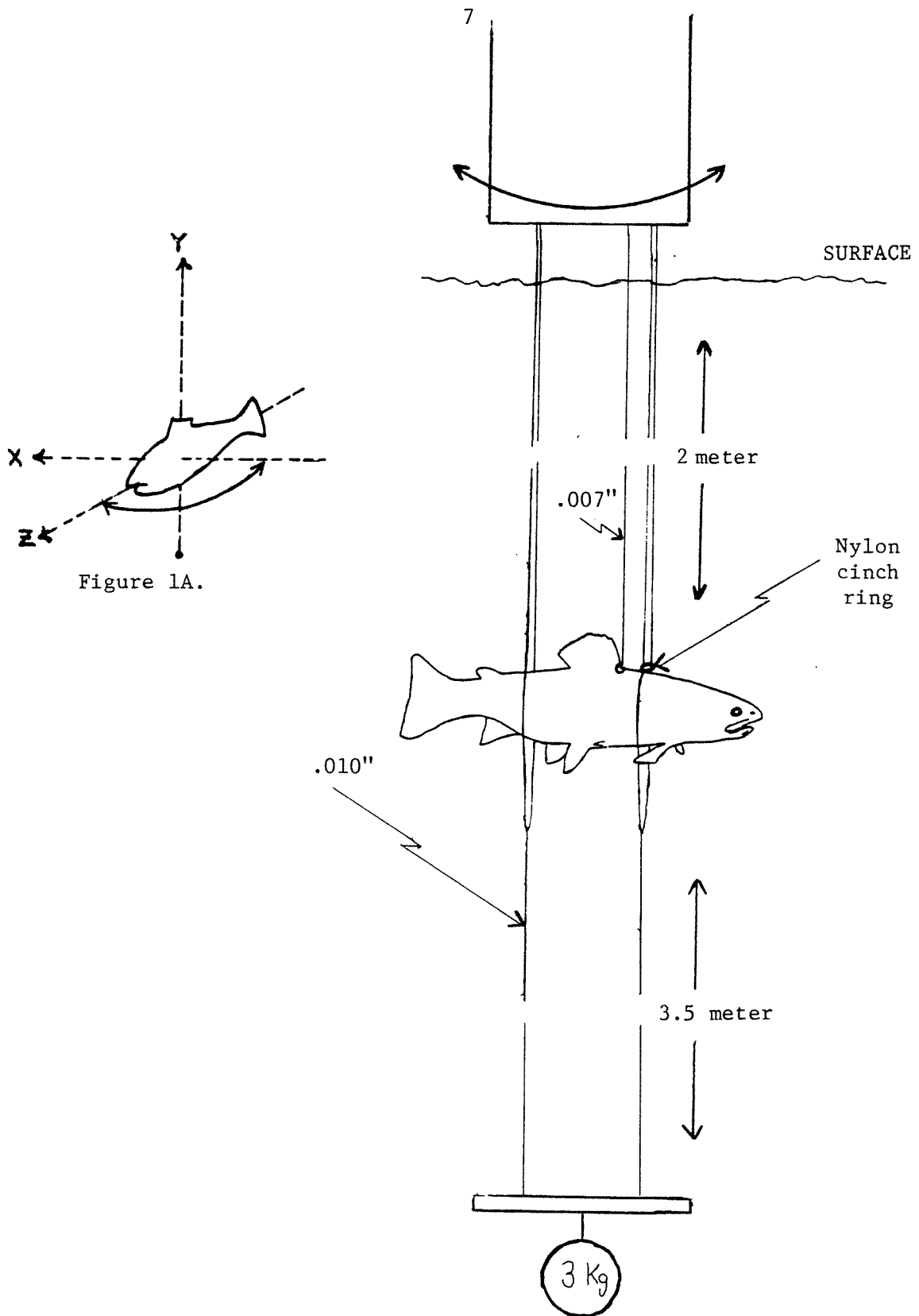


Figure 1. Monofilament line harness used to suspend and rotate fish for acoustic measurements. Figure 1A depicts rotation in the yaw (x,z) plane.

tape. The data were passed through an envelope detector to remove the carrier part of the signal, and the peak envelope voltage converted to digital form on a PDP 11/45 computer using a program written by Jim Traynor of NMFS. Target strength is calculated from digitized data using equation (2), where  $TS_{ref}$  is a -30 dB simulated acoustic signal and  $V_{ref}$  is the digital form of the peak detected voltage received from the simulation signal. The digital output for  $V_{ref}$  had a two-percent coefficient of variation.

From the analysis of the data, it was discovered that tape saturation had occurred during the measurements at side aspect, where echo intensity is greatest. Side aspect target strength data were recovered from the polar plots which have considerably higher dynamic range. The method is described in Appendix B.

## RESULTS AND DISCUSSION

A polar plot of the fish harness alone is given in Figure 2; the harness echo level was at least 25 dB below the side aspect echo level from fish, indicating minimal interference. Figure 3 shows a ping-pong ball standard target suspended within the harness, which maintained its uniform circular directivity with rotation. Figure 4 is a histogram of the ping-pong ball (radius = 1.87 cm) target strength measurements; the mean and standard deviation of the measurements are -38.6 and 0.7 dB, respectively. Drew (1980) obtained a -39.1 dB mean value for similar ping-pong ball targets, using the dual beam target strength measurement method. In summary, interference from the harness was negligible from all angles of rotation.

Polar plots of fish directivity at 420 kHz (Figures 5 through 8) showed, as expected, strong dependence of target strength on orientation. Maximum observed side aspect target strength was as high as -17 dB for fish greater than 50 cm. However, the sector of maximum target strength was approximately 15° of rotation in the yaw plane which includes the range of shift of the axis of the ascending fish. Mean side aspect target strength was 7-8 dB lower than corresponding maximum values; a data summary is presented in Table 1.

Pronounced variation is seen in the plots made at 420 kHz, due to interference from slight body motion and small changes in aspect which will cause range separation of the order of a wavelength. Figure 9 is a plot made at 120 kHz for comparison. Fish sound scattering directivity at 120 kHz is less variable than at 420 kHz. However, mean smoothed fish directivity (mean target strength in 10° sector of rotation) is more uniform at 420 kHz than at 120 kHz. Similar tendencies were found in dorsal aspect measurements of

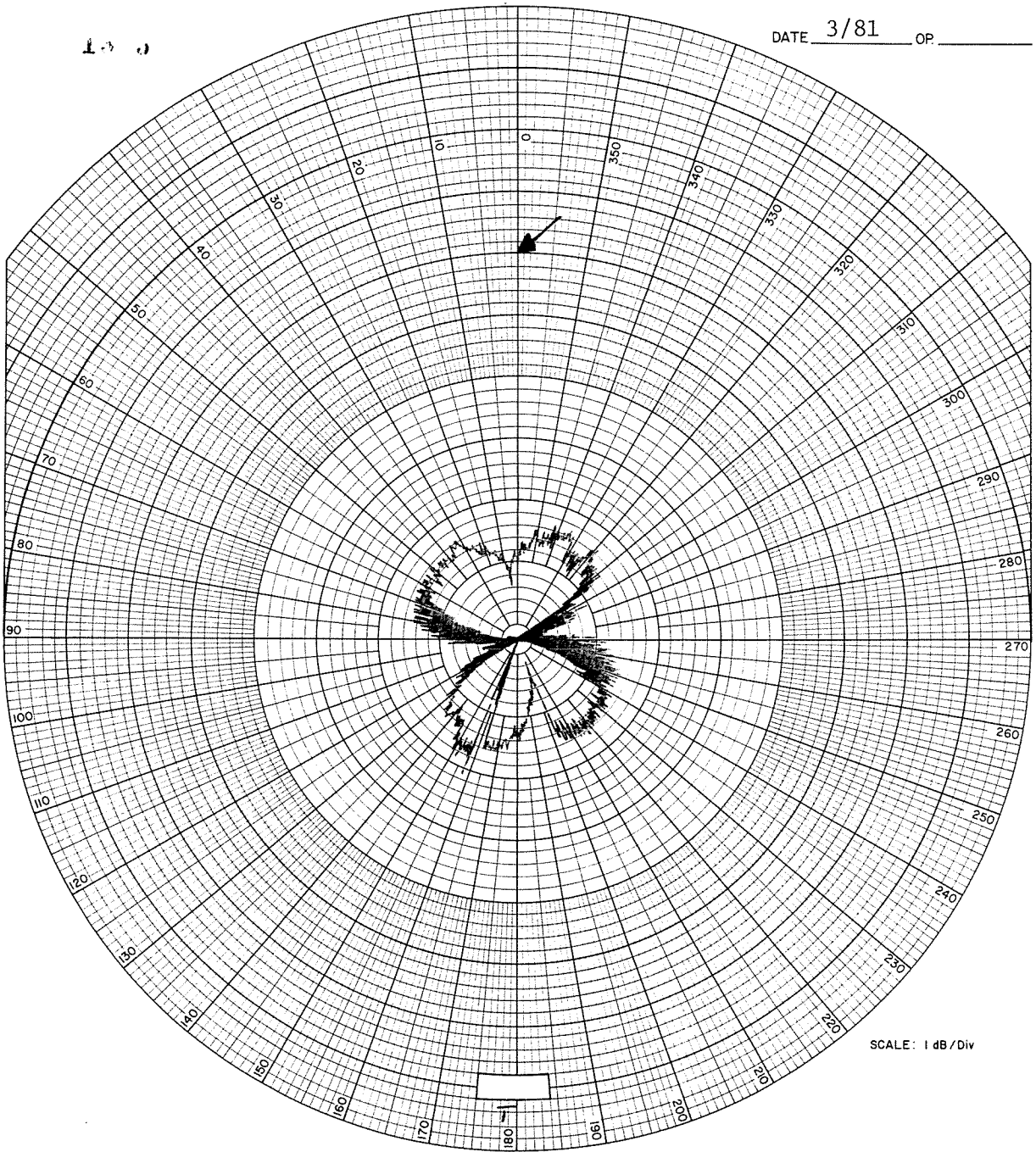


Figure 2. Polar plot (420 kHz) of 360° rotation of the monofilament fish harness. Arrow denotes -28 dB target strength; noise floor is therefore approximately -50 dB.

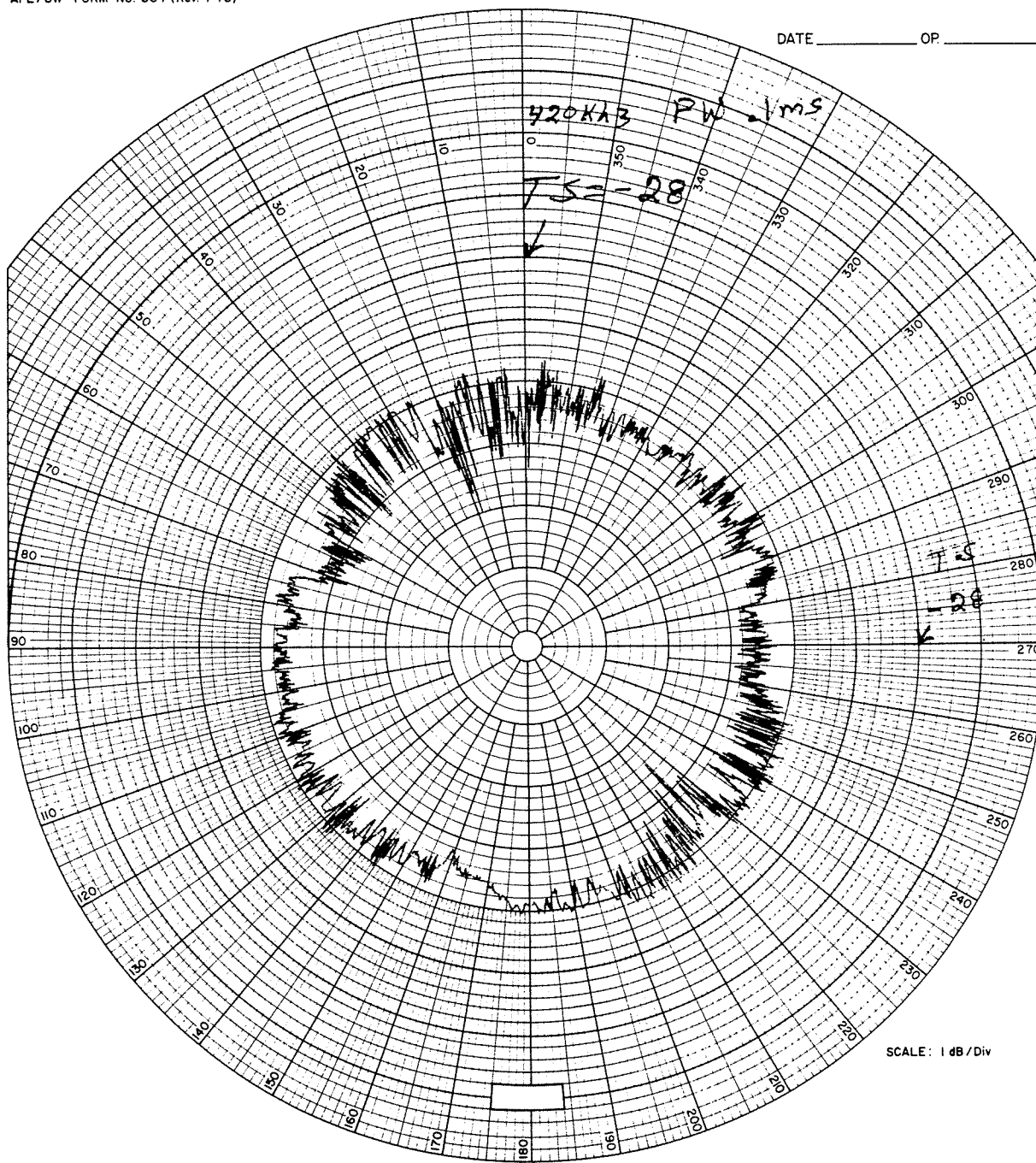
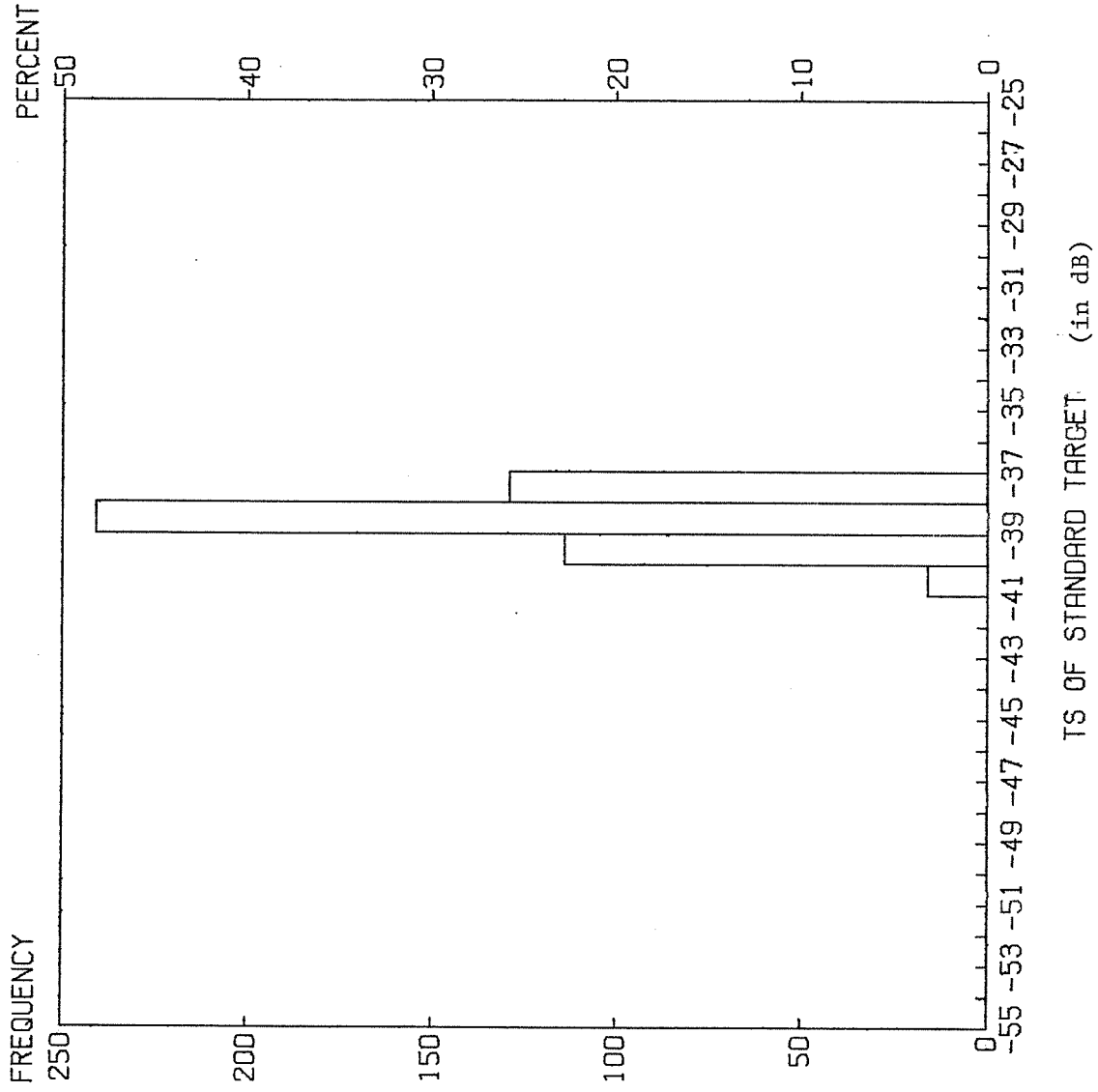
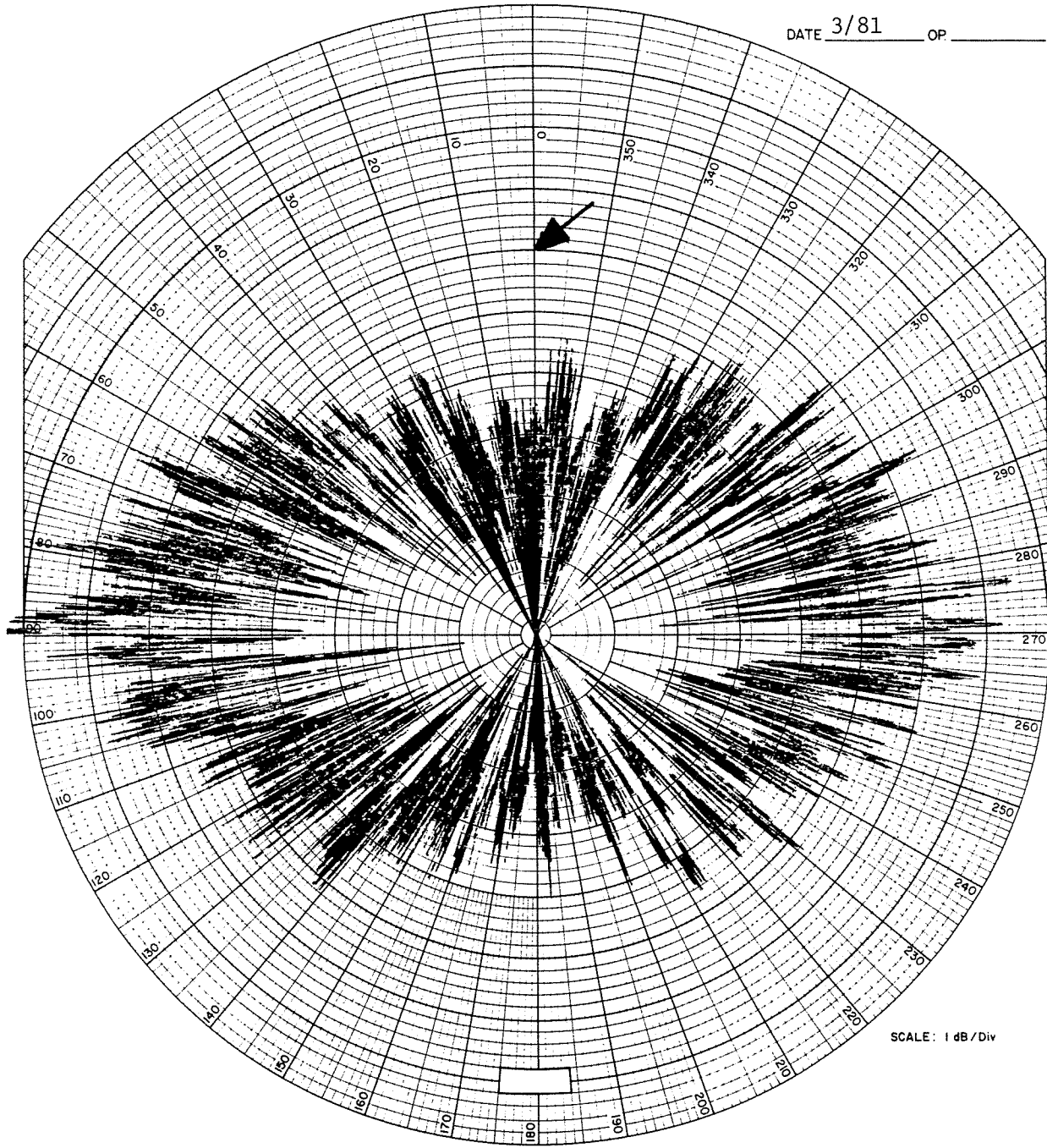


Figure 3. Polar plot (420 kHz) of standard ping-pong ball target suspended within fish harness.



TS (-38.62, .6998) 500 VALUES

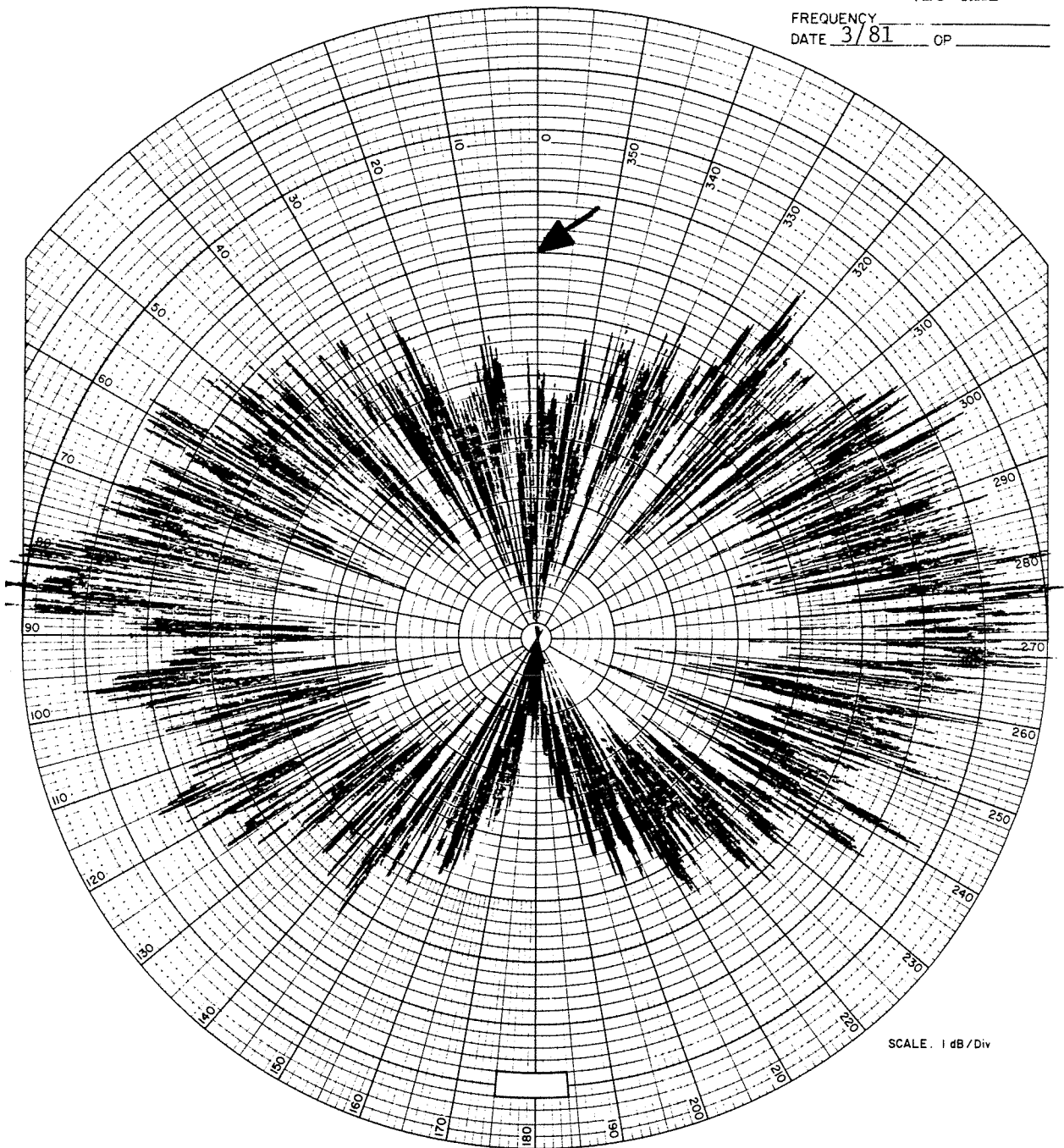
Figure 4. Ping-pong ball target strength measurements. Sample mean and standard deviation are given above.



0° = HEAD ASPECT    90° = SIDE ASPECT    180° = TAIL ASPECT

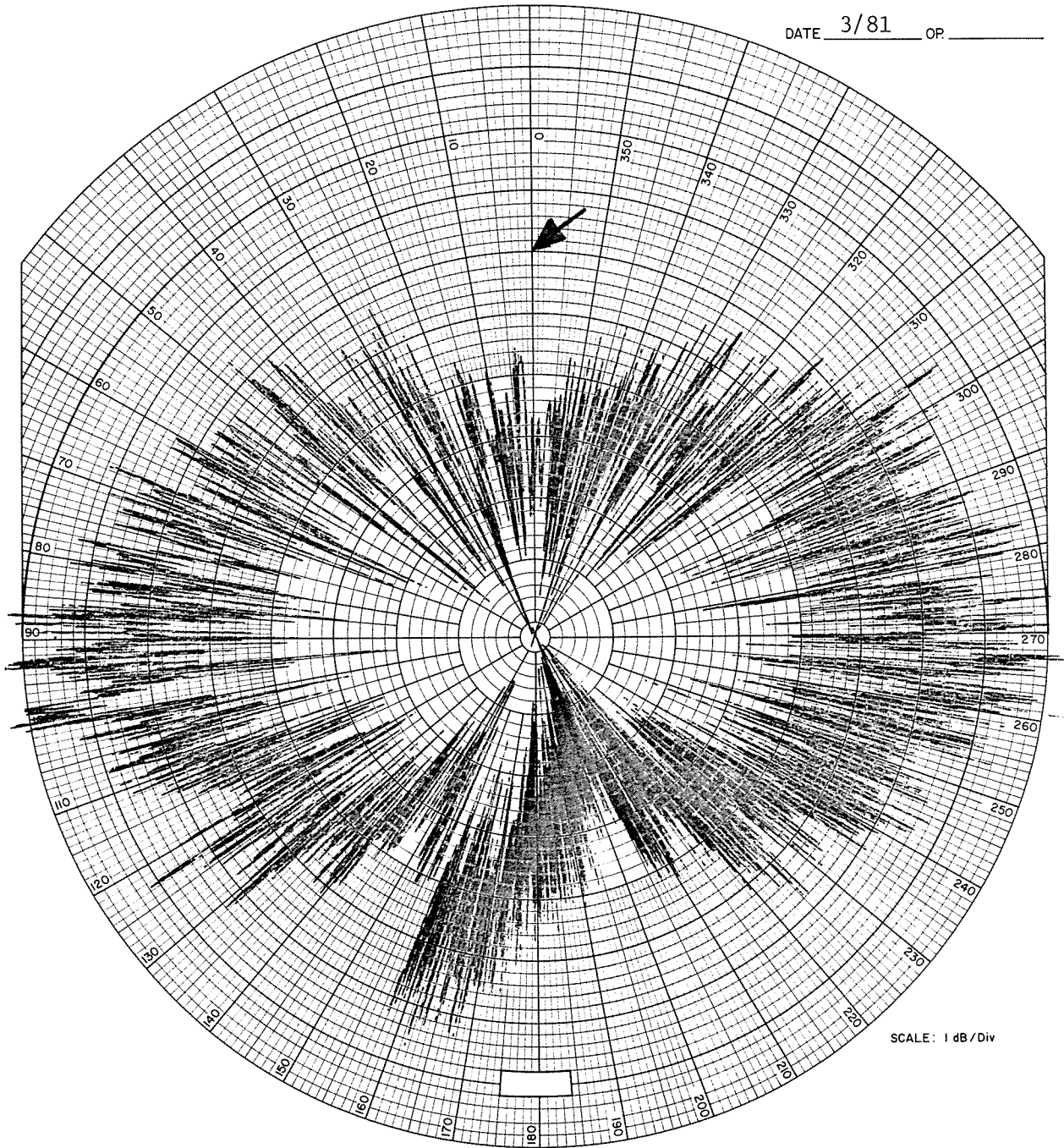
Figure 5. Polar plot (420 kHz) of fish directivity in the yaw plane for fish No. 1. Arrow denotes -28 dB target strength.

420 kHz

FREQUENCY \_\_\_\_\_  
DATE 3/81 CP \_\_\_\_\_

0° = HEAD ASPECT    90° = SIDE ASPECT    180° = TAIL ASPECT

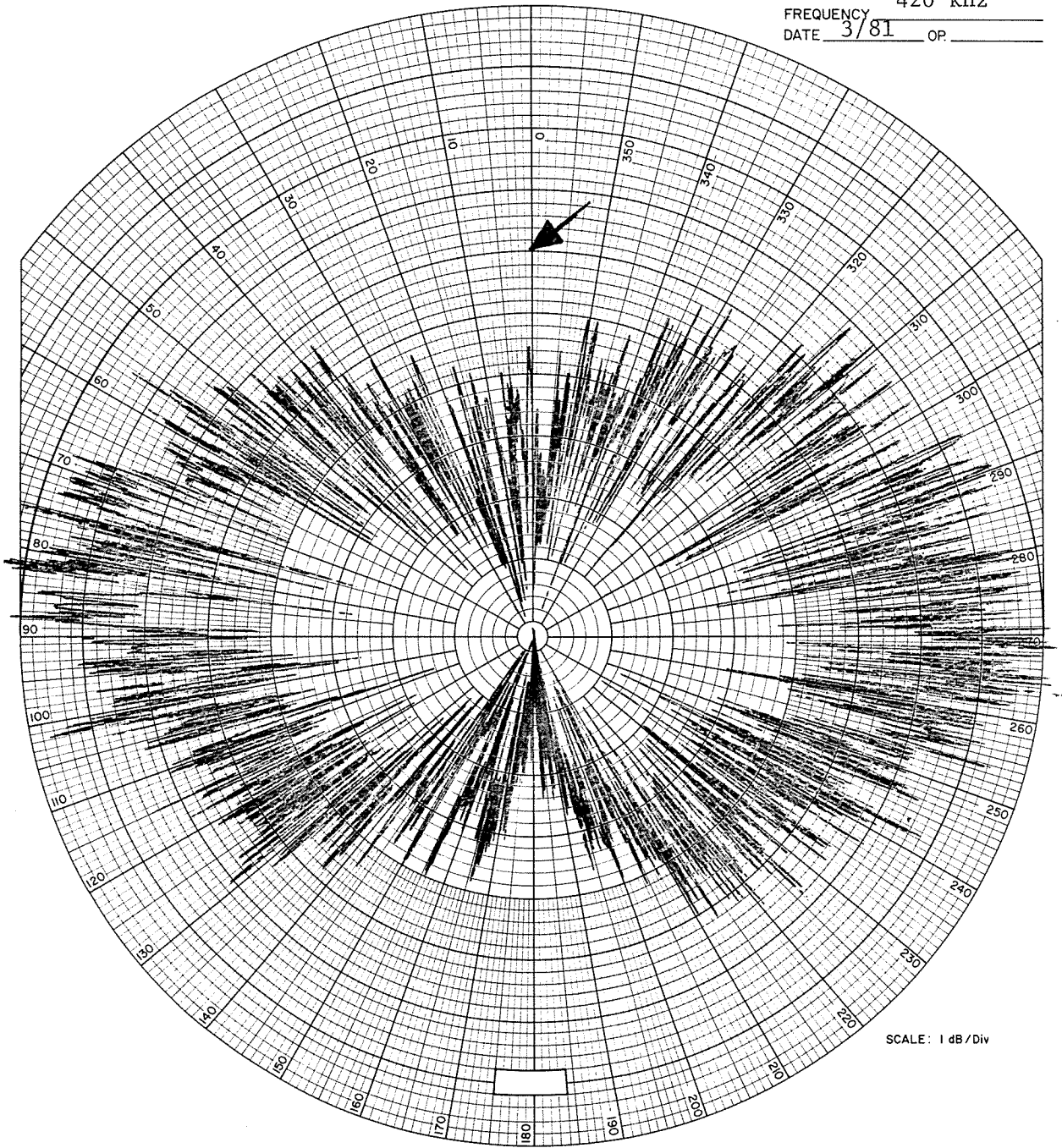
Figure 6. Polar plot (420 kHz) of fish directivity in the yaw plane for fish No. 2. Arrow denotes -28 dB target strength.



0° = HEAD ASPECT    90° = SIDE ASPECT    180° = TAIL ASPECT

Figure 7. Polar plot (420 kHz) of fish directivity in the yaw plane for fish No. 3. Note change in target strength variation at 160°, where fish began recovery from anesthesia. Arrow denotes -28 dB target strength.

FREQUENCY 420 kHz  
DATE 3/81 OP. \_\_\_\_\_



0° = HEAD ASPECT    90° = SIDE ASPECT    180° = TAIL ASPECT

Figure 8. Polar plot (420 kHz) of fish directivity in the yaw plane for fish No. 6. Arrow denotes -28 dB target strength.

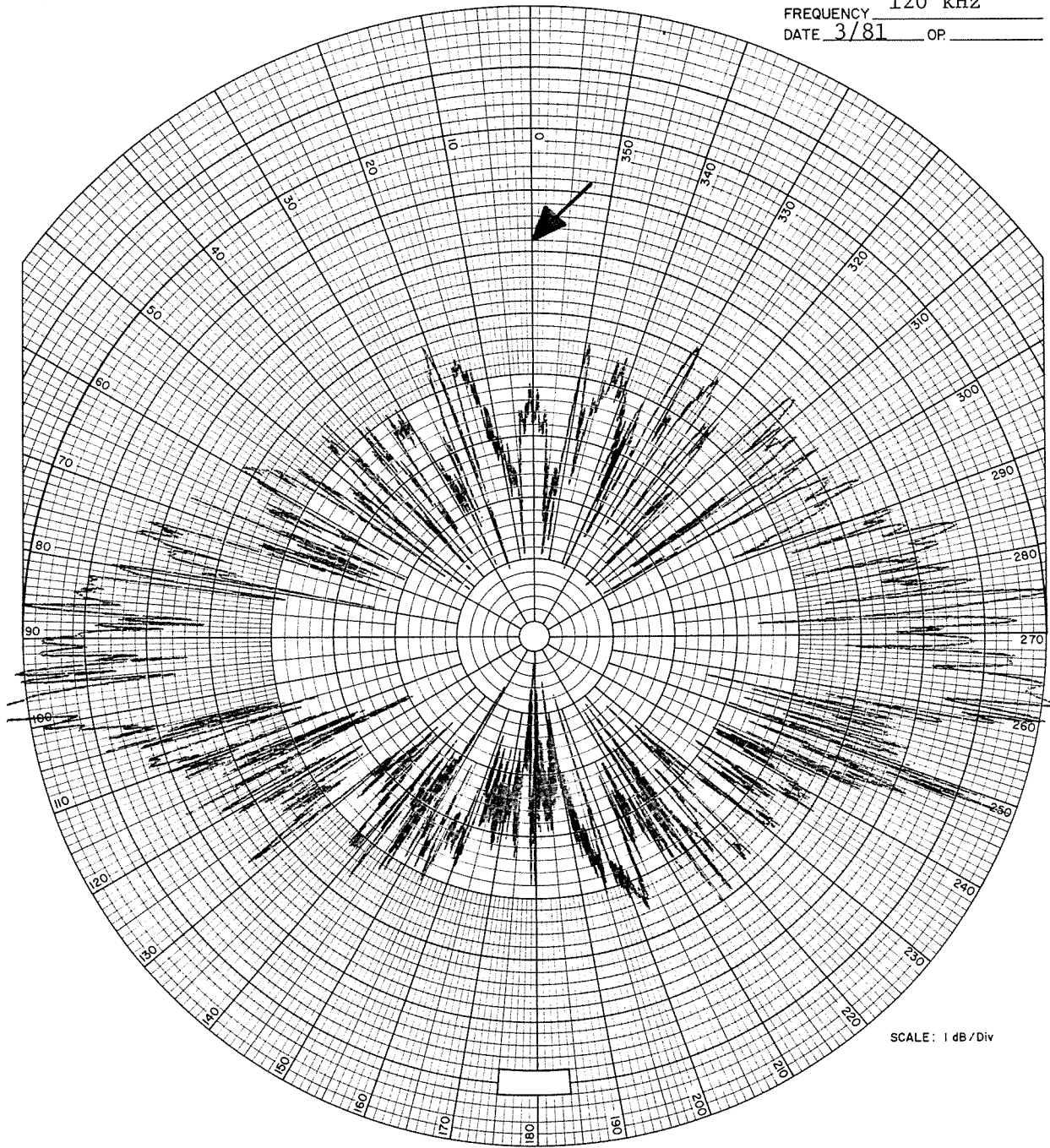
Table 1. Species, length, and weight of salmonid targets, with corresponding mean and maximum observed side aspect target strength.

Fish	Species	Length (cm)	Weight (kg)	Mean TS <sup>1</sup>	Max. observed TS <sup>2</sup>
1	<u>Salmo clarki</u>	40	0.65	-26.6	-18
2	<u>Salmo gairdneri</u> (Steelhead)	52	1.92	-25.0	-17
3	<u>Salmo gairdneri</u>	55	2.33	-25.9	-17
4	<u>Salmo gairdneri</u>	56	2.64	-24.7	-17
5	<u>Salmo gairdneri</u>	57	2.62	-23.6	-17
6	<u>Salmo gairdneri</u>	61	3.10	-24.0	-17

<sup>1</sup> Mean side aspect target strength from the 10° sector of maximal target strength as determined from polar plots.

<sup>2</sup> Precision of polar plot scale is 1 dB.

FREQUENCY 120 kHz  
DATE 3/81 OP. \_\_\_\_\_



0° = HEAD ASPECT    90° = SIDE ASPECT    180° = TAIL ASPECT

Figure 9. Polar plot (120 kHz) of fish directivity in the yaw plane for fish No. 5. Arrow denotes -35 dB target strength.

of trout at 38 kHz and 120 kHz by Carlson (1979). More uniform fish sound scattering directivity is desired for river sonar applications, where the instantaneous aspect of the fish is usually unknown. A plot of the smoothed fish directivity at 420 kHz, for the 40 cm, 52 cm and 61 cm fish is presented in Figure 10.

Note the decrease in target strength at 120 kHz. Although the dB scale for the 120 kHz plot was not confirmed by calibration, target strength measurements at 120 kHz were noticeably less than those at 420 kHz, perhaps by 5 dB. This is expected; at higher frequencies additional components of the fish such as scales, fin rays, spines, etc., become significant scatterers and contribute to the echo.

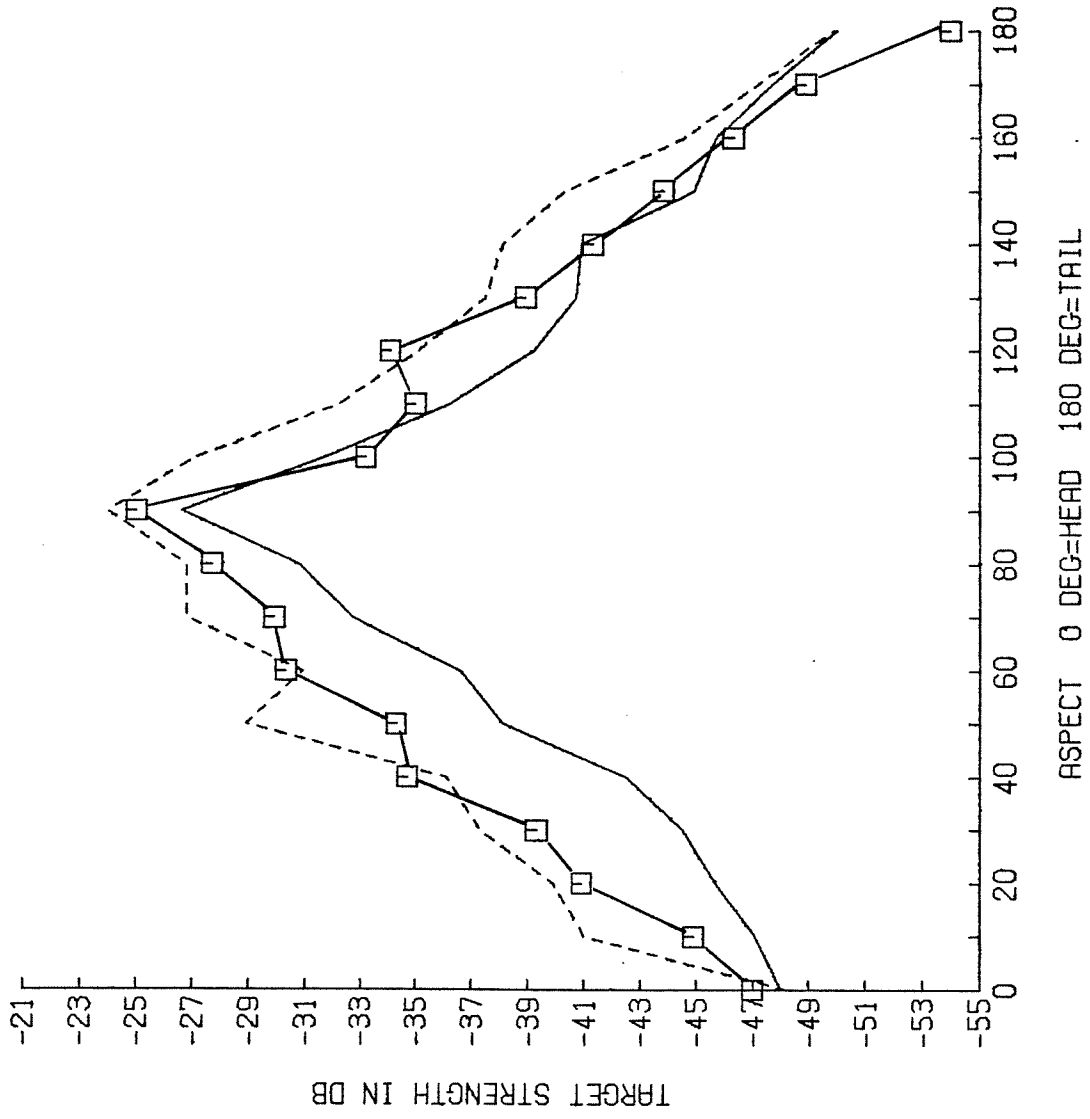
The target strength/fish length relation was consistent with the observed trend of increasing target strength with fish length. More specific conclusions would not be appropriate, as only six fish lengths were used. The plot of the regression of target strength with fish length is presented in Figure 11.

#### Target Strength Statistics

Figure 12 is a histogram of peak detected echo voltage from a 56 cm fish positioned 45° off head aspect (corresponding to 45° or 315° on polar plots). A chi-square goodness-of-fit test was performed to test the following hypothesis:

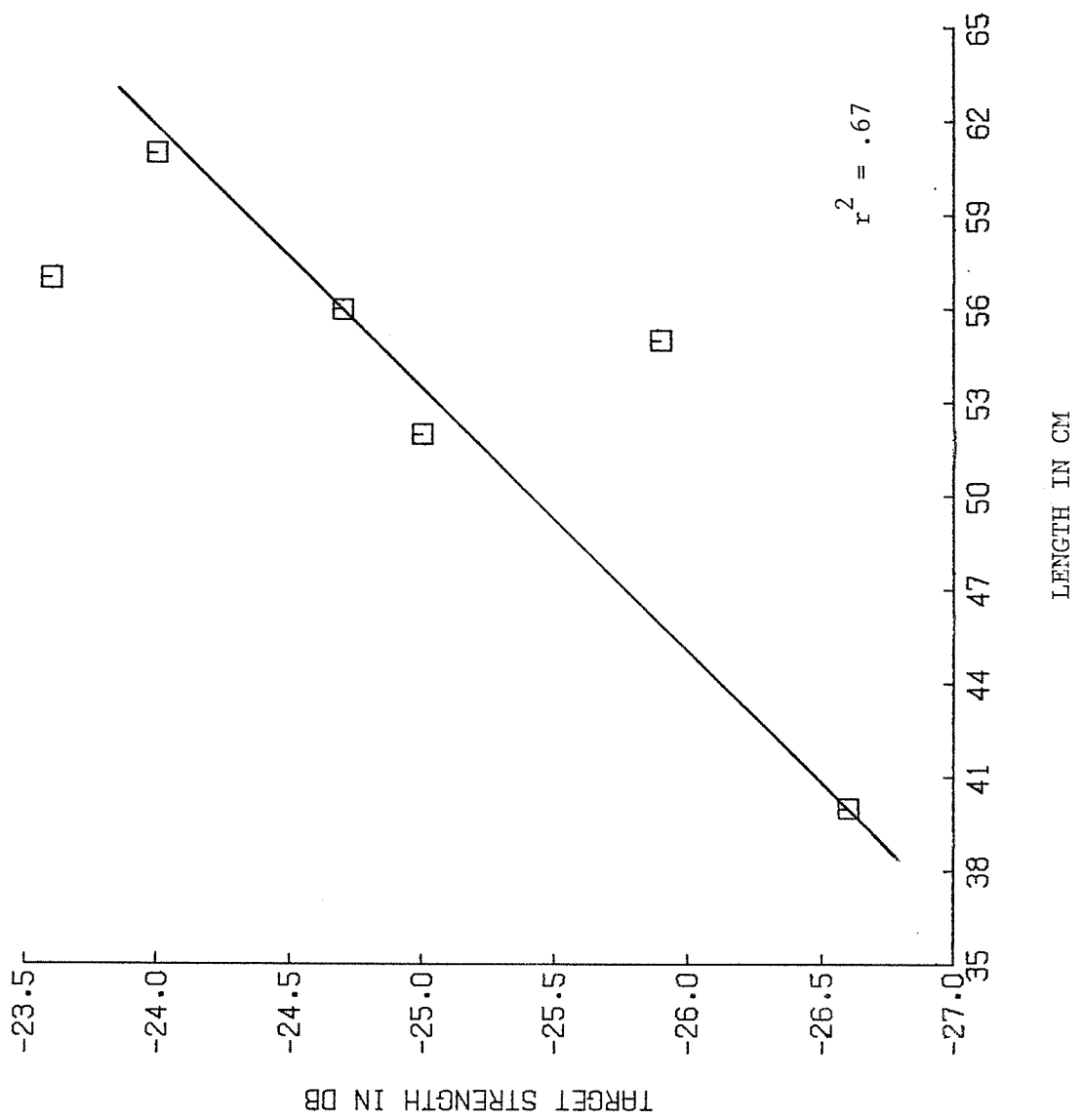
$H_0$ : Peak detected voltage is Rayleigh distributed using maximum likelihood estimate from the sample data.

$H_1$ : Peak detected voltage is not Rayleigh distributed.



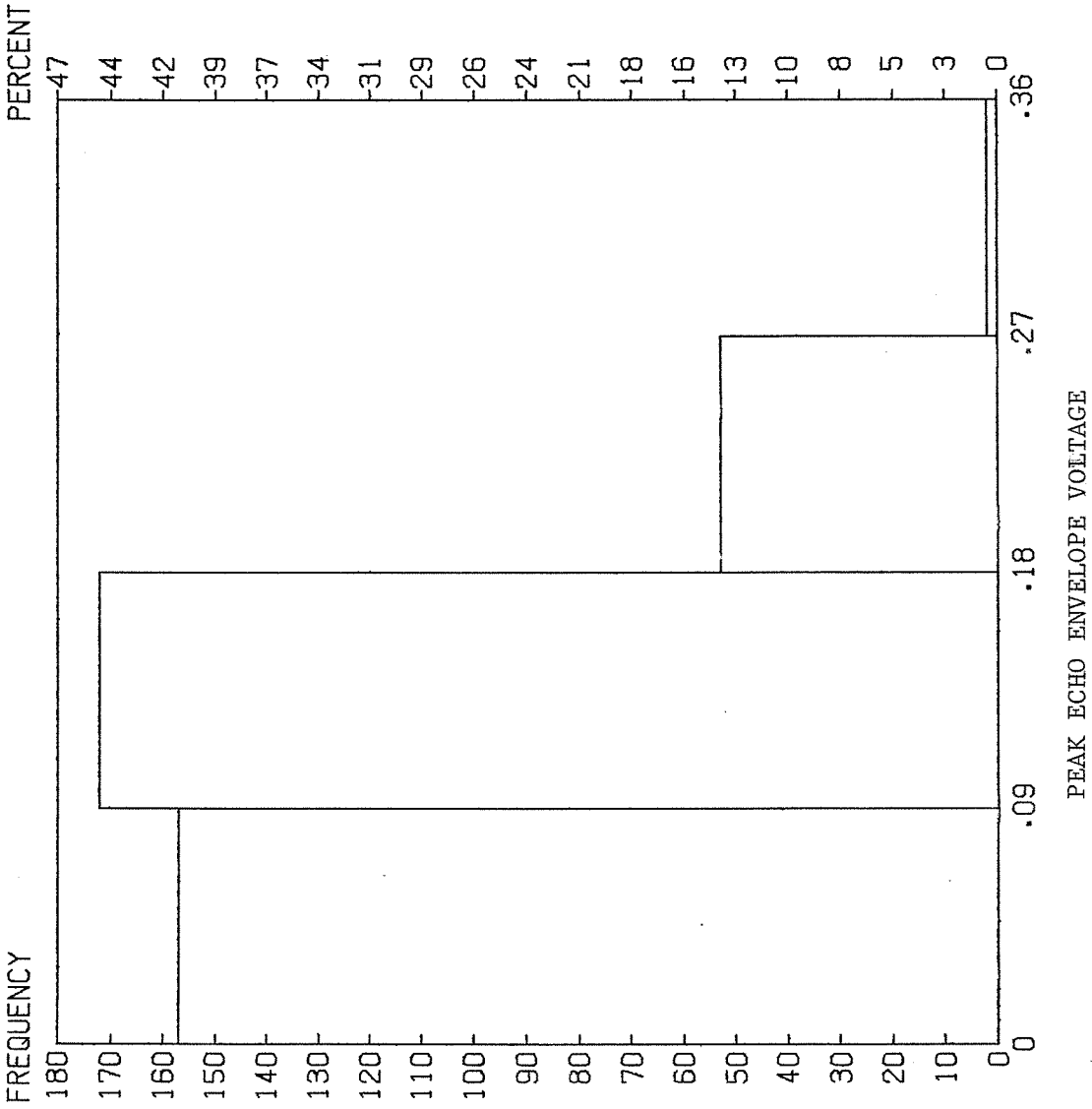
LINE = fish No. 1 (40 cm) SYMBOL = fish No. 2 (52 cm) DASH = fish No. 6 (61 cm)

Figure 10. Plot of mean target strength in 10° increments.



□ LENGTH VERSUS TS 6 VALUES

Figure 11. Regression of target strength with fish length.



AMP (.1099, .06231)

Figure 12. Peak echo envelope voltage measurements, from fish No. 3 positioned at 45° aspect. Sample mean and standard deviation are given above.

The result was not significant ( $.25 < p < .50$ ), and the null hypothesis was therefore accepted.

Using equation (2), the above digital amplitude data are transformed to equivalent target strength with resulting histogram presented in Figure 13. Given that peak detected voltage (or equivalently  $\sqrt{\delta_{bs}}$ ) is Rayleigh distributed, the corresponding probability density function for target strength is

$$f(t) = \frac{e^{\frac{2t}{k_2}}}{a} \cdot C_1 \cdot \exp \left\{ \frac{-C_2}{a} e^{\frac{2t}{k_2}} \right\} \quad (4)$$

where

$t$  = argument of the random variable TS

$a$  = single Rayleigh parameter

$k_2 = 20 \log e$

$C_1$  and  $C_2$  are system-dependent constants.

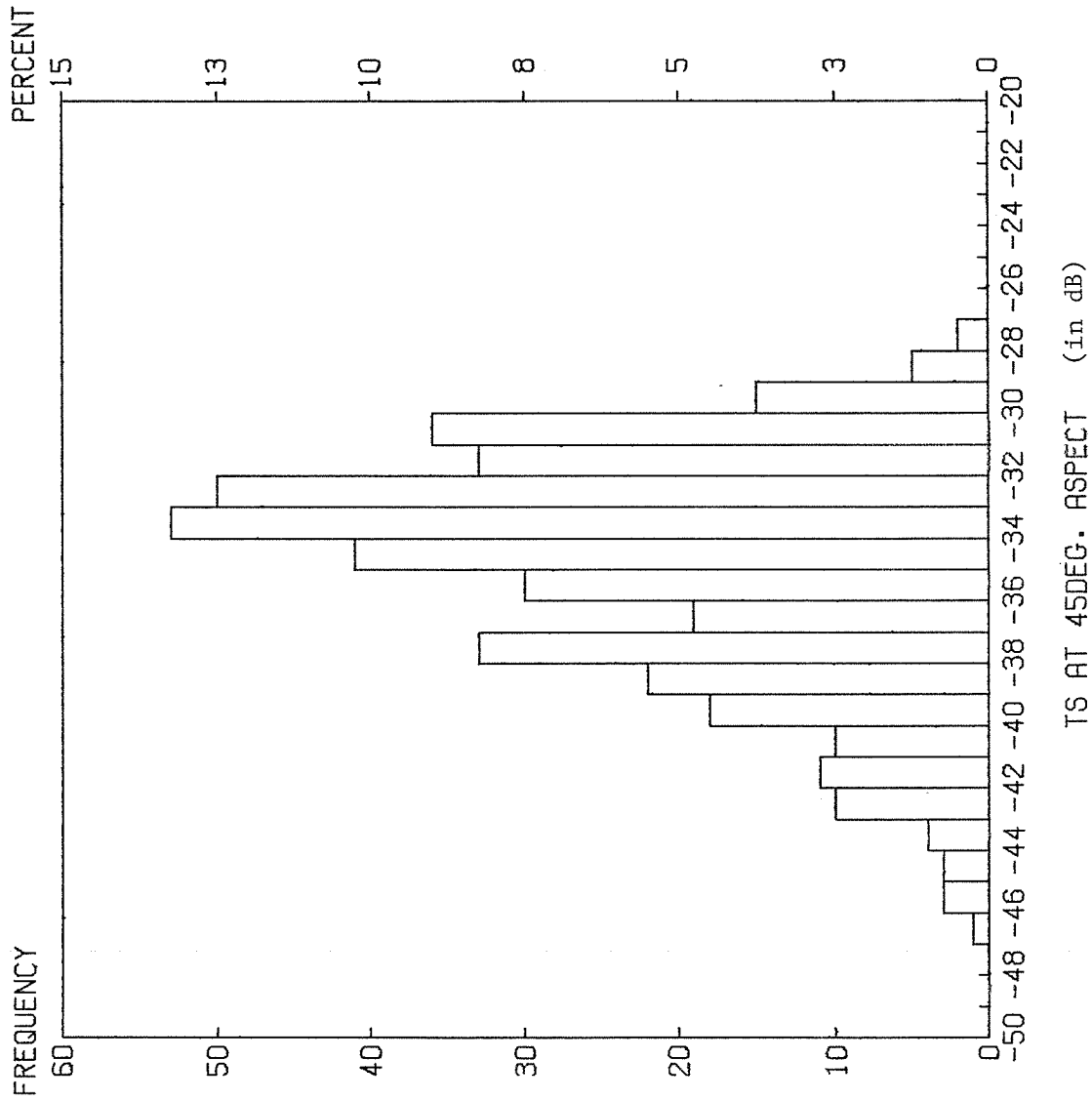
The target strength probability distribution function follows from integrating the density function,

$$F(t) = 1 - \exp \left\{ \frac{-C_2}{a} e^{\frac{2t}{k_2}} \right\} \quad , \quad (5)$$

such that

$$F(\xi) = \text{Probability} \{ \text{TS} \leq \xi \} \quad .$$

(Derivation of the above is found in Appendix C).



TS (-34.97,3.815)

Figure 13. Target strength values corresponding to data in Figure 12. Sample mean and standard deviation are given above.

Histograms of side aspect target strength values obtained from the polar plots (as per Appendix B) are presented in Figures 14 through 19. The solid line is a maximum likelihood fit of the target strength probability density function given the Rayleigh assumption. A chi-square goodness-of-fit test was performed on the data from Figures 14-19 to test the following hypothesis:

$H_0$ : Target strength is distributed according to equation (5) using maximum likelihood estimate from sample data.

$H_1$ : Target strength is not distributed according to equation (5).

The null hypothesis was accepted in all cases except for the data in Figure 19; sampling artifact is assumed to have caused the significant chi-square statistic in this case. Results of the tests are presented in Table 2.

The results of the goodness-of-fit tests strongly suggest that the Rayleigh model is valid, and accordingly equations (4) and (5) are appropriate statistical models for target strength. The expected value of target strength is therefore

$$E[t] = 4.3429 \ln(a) + .5033 + k_1, \quad (6)$$

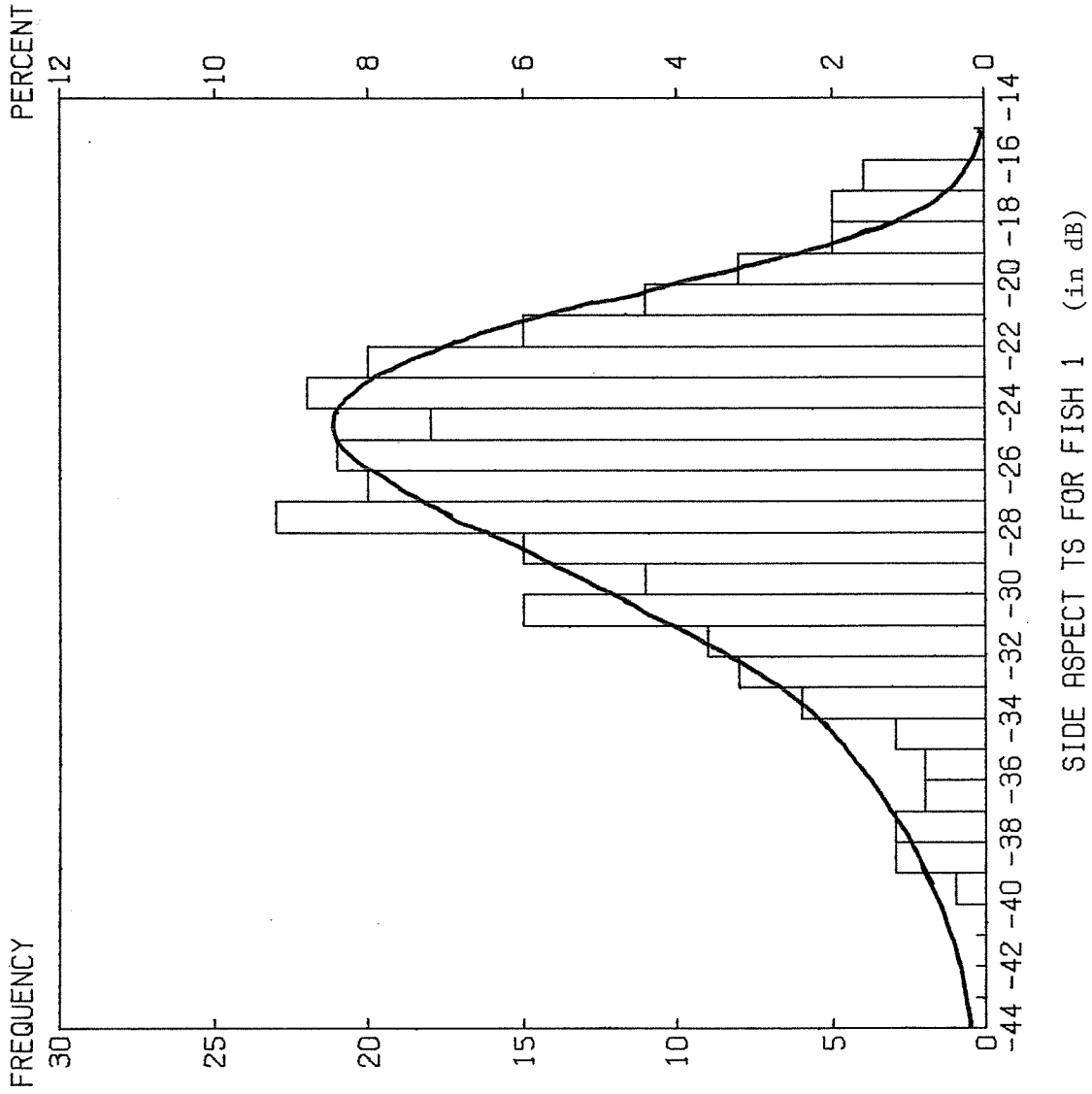
where

$a$  = density function parameter

$$k_1 = -10 \log 4\pi$$

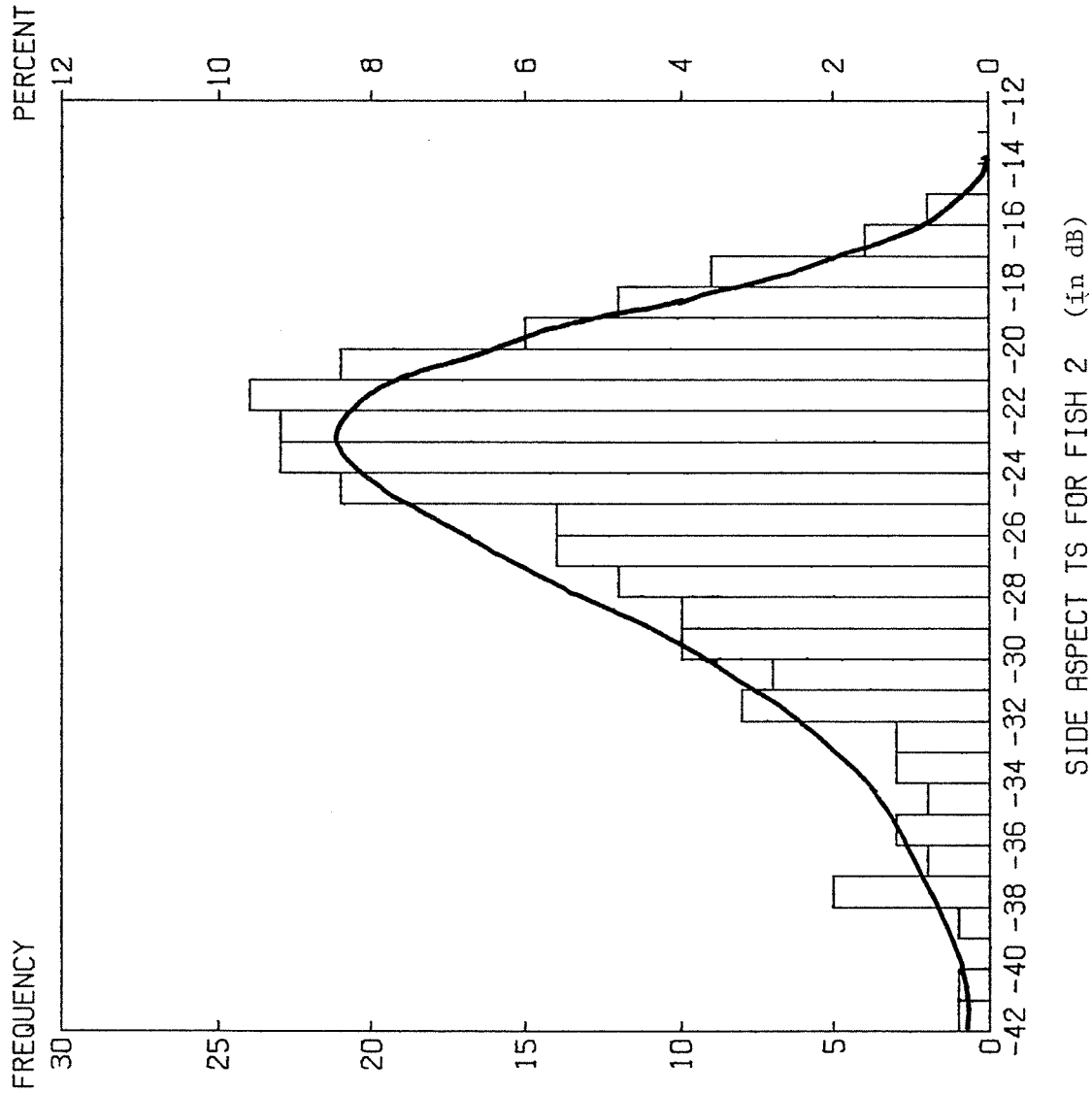
Target strength variance follows from

$$E[t^2] = \frac{k_2^3}{8} \frac{C_1}{C_2} \left[ \frac{\pi^2}{6} + \left( C_E + \ln \left( \frac{C_2}{a} \right) \right)^2 \right] \quad (7)$$



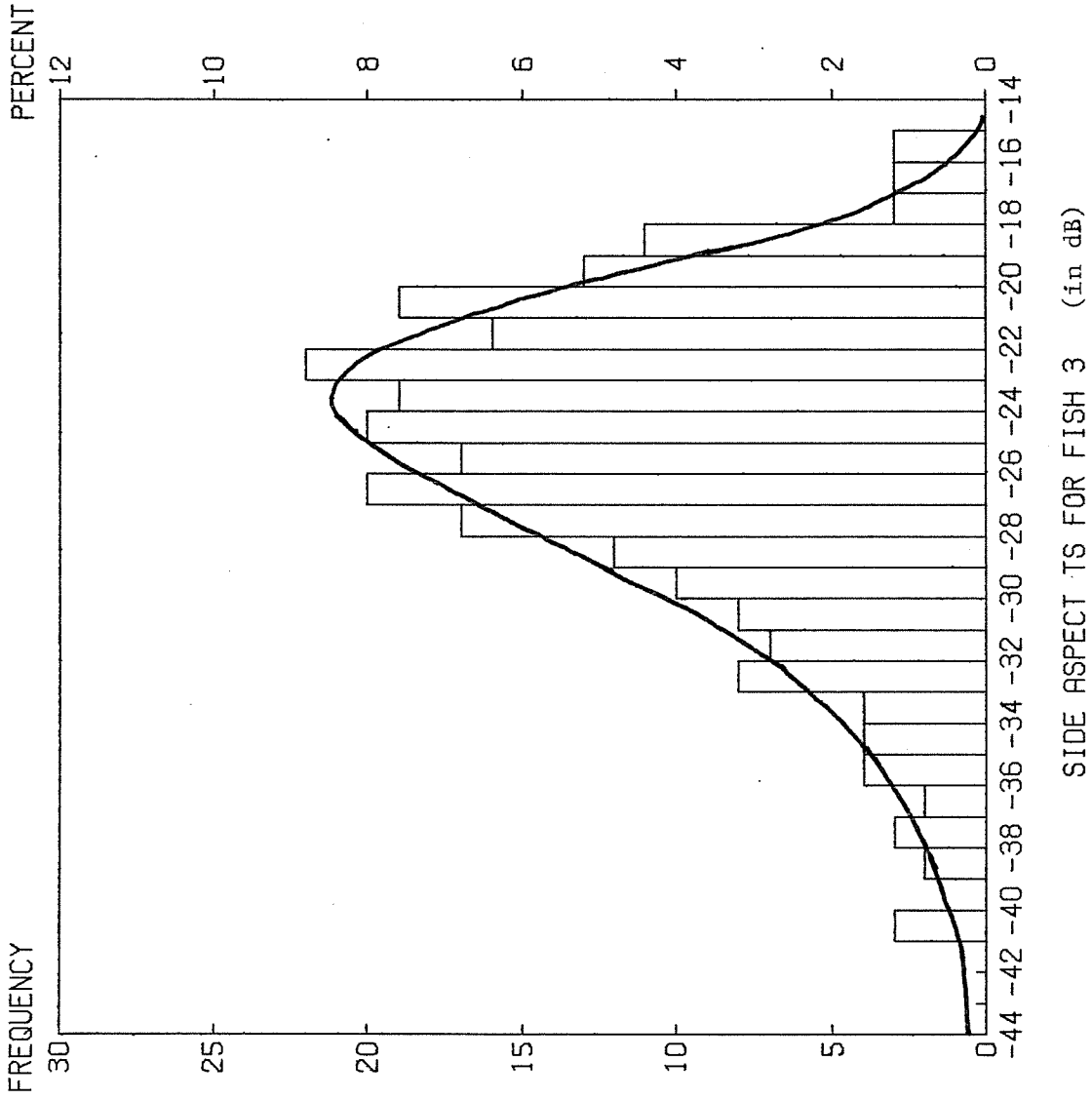
TS (-26.6, 4.745) 250 VALUES

Figure 14. Side aspect target strength measurements. Solid line is maximum likelihood fit of target strength probability density function, where  $\hat{\mu} = -26.6$  and  $\hat{\sigma} = 4.745$ . Sample mean and standard deviation are given above.



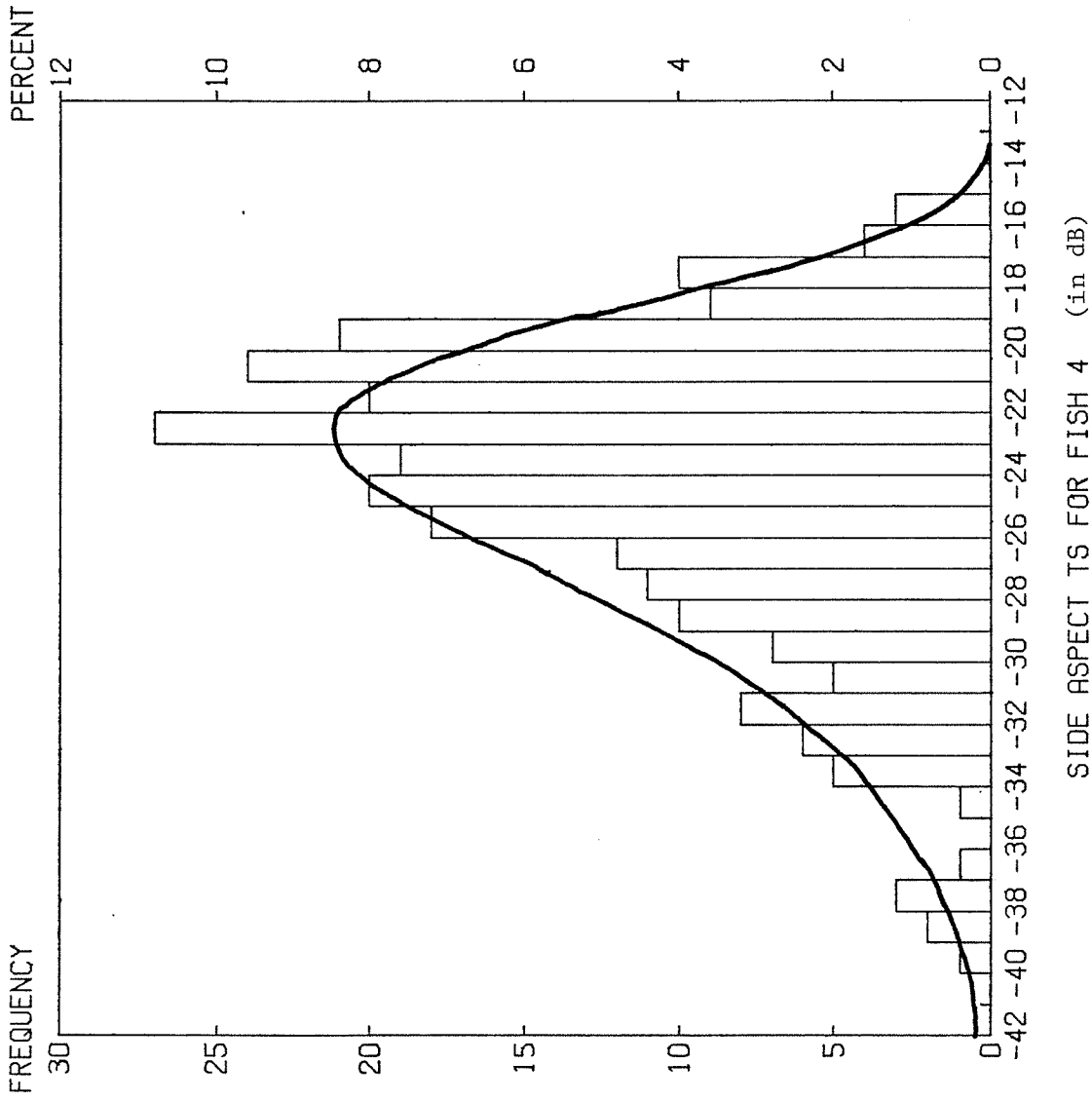
TS (-25.08, 5.084) 250 VALUES

Figure 15. Side aspect target strength measurements. Solid line is maximum likelihood fit of target strength probability density function, where  $\hat{\mu} = -25.08$  and  $\hat{\sigma} = 5.084$ . Sample mean and standard deviation are given above.



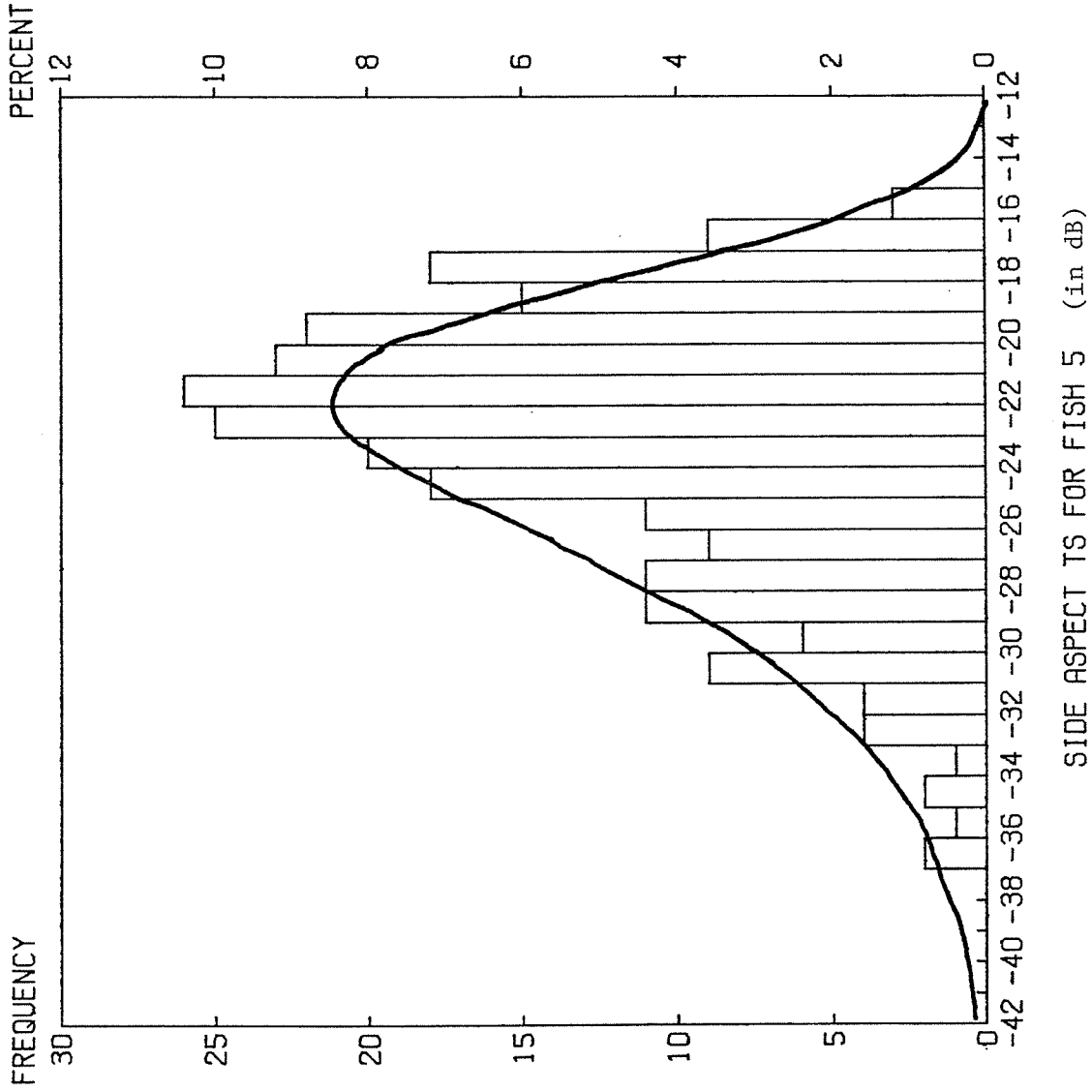
TS (-25.94, 5.161) 250 VALUES

Figure 16. Side aspect target strength measurements. Solid line is maximum likelihood fit of target strength probability density function, where  $\hat{\alpha} = .0279$ . Sample mean and standard deviation are given above.



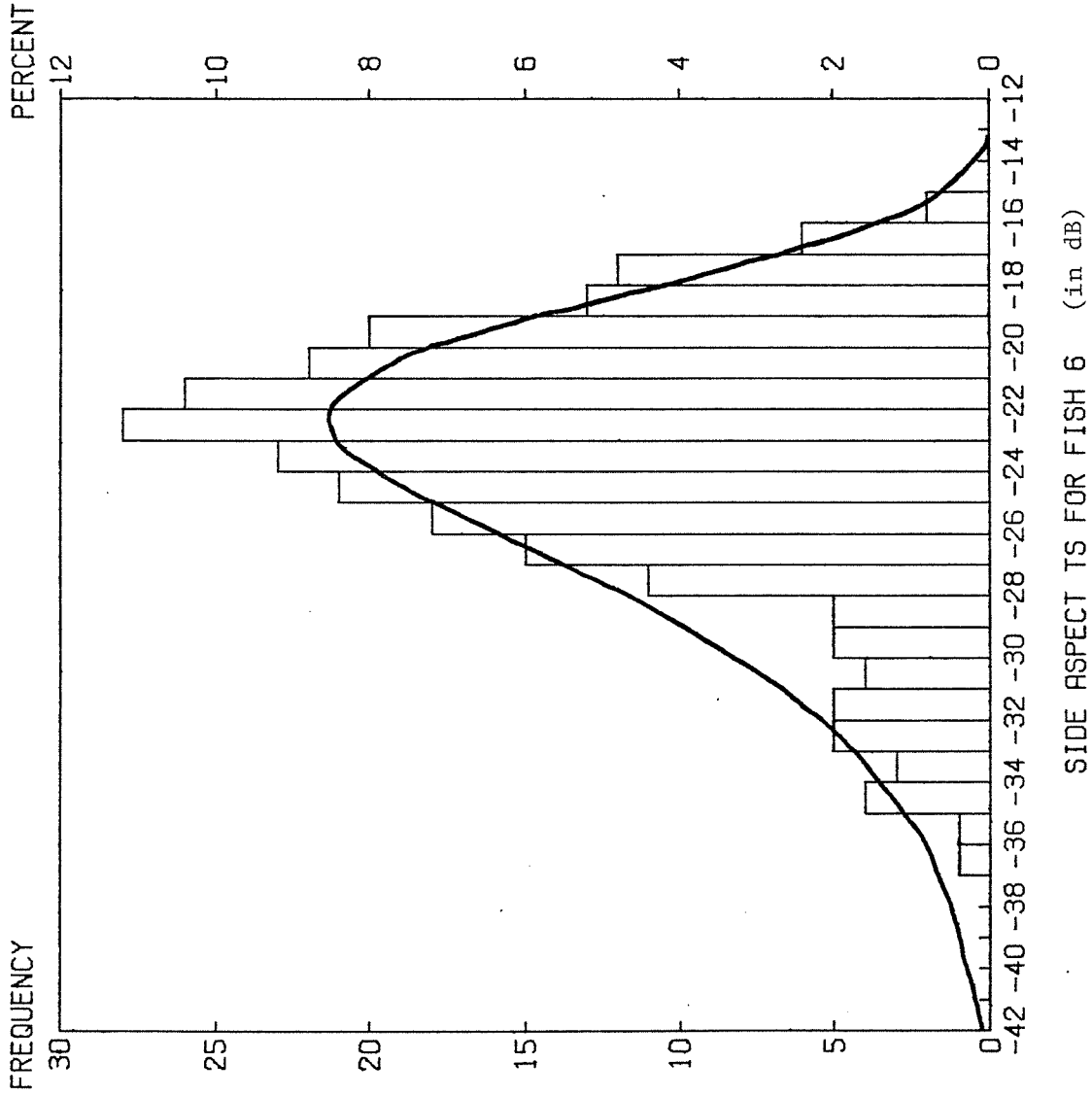
TS (-24.66, 4.826) 247 VALUES

Figure 17. Side aspect target strength measurements. Solid line is maximum likelihood fit of target strength probability density function, where  $\hat{\mu} = -24.66$  and  $\hat{\sigma} = 4.826$ . Sample mean and standard deviation are given above.



TS (-23.60, 4.462) 250 VALUES

Figure 18. Side aspect target strength measurements. Solid line is maximum likelihood fit of target strength probability density function, where  $\hat{\mu} = -23.60$  and standard deviation are given above.



TS (-23.97, 4.277) 250 VALUES

Figure 19. Side aspect target strength measurements. Solid line is maximum likelihood of fit of target strength probability density function, where  $\hat{\mu} = -23.97$ ,  $\hat{\sigma} = 4.277$ . Sample mean and standard deviation are given above.

Table 2. Results of chi-square goodness-of-fit tests on data from Figures 14-19.

Fish	Length (cm)	Probability of chi-square statistic
1	40	.10 < p < .25
2	52	.05 < p < .10
3	55	.25 < p < .5
4	56	p > .5
5	57	.25 < p < .5
6 <sup>1</sup>	61	.01 < p < .025

<sup>1</sup> Significant chi-square statistic.

where  $k_2$ ,  $C_1$ ,  $C_2$  are defined in equation (4).

$$C_E = .577215 \quad (\text{Euler's constant})$$

thus

$$\text{Var}[t] = E[t^2] - \{E[t]\}^2 \quad (8)$$

Derivation of the above is found in Appendix D.

Target strength statistics depend on the single Rayleigh parameter  $a$ , which has dimensions of (meter)<sup>2</sup> if variable  $Z$  (from equation 5) denotes square root of backscattering cross-section, or (voltage)<sup>2</sup> if  $Z$  denotes echo envelope amplitude. The maximum likelihood estimate ( $\hat{a}$ ) from sample data for fish 5 is .0416, applying  $\hat{a}$  to equations (6), (7) and (8) gives

$$\overline{\text{TS}} = -24.3 \text{ dB}$$

$$\text{S.D. TS} = 5.3 \text{ dB}$$

This compares with sample mean and standard deviation of -23.6 dB and 4.5 dB. Bias inherent in sampling method (Appendix B) will tend to reduce variance, and  $\pm 5$  dB is a more likely standard deviation.

## SUMMARY AND CONCLUSIONS

Fish sound scattering directivity and target strength of salmonids have been studied in regard to the application of hydroacoustic techniques for assessing anadromous salmon runs. Measurements were made at 420 kHz, the indicated operating frequency for riverine sonar. Maximum observed side aspect target strength for 55-60 cm salmonids was -17 dB; sample mean and standard deviation were approximately -25 dB and 4.5 dB, respectively.

Polar plots of fish directivity made at both 420 kHz and 120 kHz show expected dependence of fish target strength on fish orientation in sonar beam. The polar plots have a general pattern which follows the decrease in back-scattering cross-section as the fish rotates from minimum head-tail aspect to maximum side aspect. A mean target strength value for each 10° sector of rotation in the yaw plane was extracted from the plots made at 420 kHz. The resulting mean smoothed fish directivity was more uniform; the more uniform fish directivity is desired for riverine sonar applications where the instantaneous fish aspect is often unknown. The sector of maximum target strength was approximately 15° of rotation.

The polar plots made at 420 kHz show large fluctuations in target strength (5-10 dB) following small changes in aspect. These fluctuations can be attributed to change in range (on the order of wavelength) from slight movement of the fish body, and to the assumption that the fish echo results from contributions of a number of discrete scattering sources with random phase. However, the echo fluctuation can be described by a univariate probability distribution, if echoes are from fixed aspect, and are not individually weighted by the transducer beam pattern (i.e. on-axis target). Explicit expressions for target

strength expected value and variance are derived from the assumption that the square root of backscattering cross-section, or its equivalent echo envelope amplitude, is Rayleigh distributed. Statistical goodness-of-fit tests on data obtained by two different methods strongly support this assumption.

## ACKNOWLEDGEMENTS

We wish to thank the following people and organizations for the additional support necessary for completion of this project. Acoustic instrumentation was provided by W. C. Acker of the BioSonics Corp. Fish and fish handling facilities were provided by W. K. Hershberger of the University of Washington School of Fisheries and Jim Mighell of National Marine Fisheries Service. Arrangements for fabrication of steel support structure for on-site fish handling were made by C. O. Dahl.

We wish to thank Tom Carlson of BioSonics for his invaluable advice during both the planning of this project and the data analysis; additional consultation from John Ehrenberg of Applied Physics Laboratory is appreciated. Thanks is extended to Jim Traynor of National Marine Fisheries Service for the use of his computer program, Gary McGlasson who was responsible for the electronics aboard the acoustics research barge, and Warner Lou for his assistance during the data collection. Review of this manuscript by Stan Murphy is greatly appreciated.

This research was also partially supported by the Washington Sea Grant Program, under the National Oceanic and Atmospheric Administration, U.S. Department of Commerce.

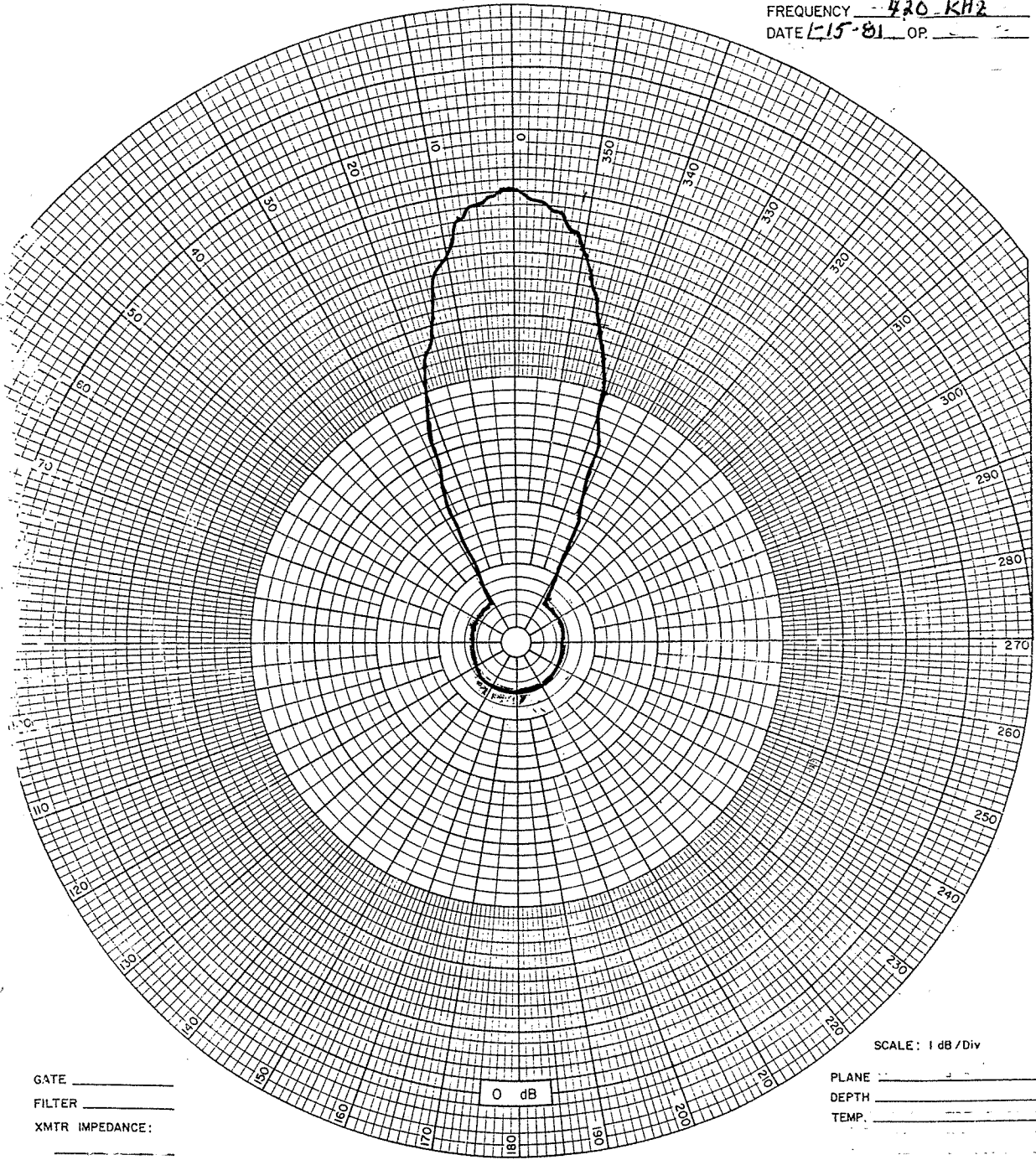
## REFERENCES

- Carlson, T. J. 1978. Near dorsal aspect hydroacoustic target properties of rainbow trout and an echo-classifier based abundance estimation method. Ph.D. thesis, Univ. of Washington, Seattle.
- Carlson, T. J. and W. C. Acker. 1979-1980. 1979-1980. Abundance estimation of migrating fish in the Quinault River. Unpublished project quarterly reports, Applied Physics Laboratory, Univ. of Washington, Seattle.
- Clay, C. S. and H. Medwin. 1977. Acoustical Oceanography: Principles and Applications. John Wiley & Sons, New York. pp. 476-482.
- Davis, A. S. 1972. Sonic assessment of salmon escapements. Anadromous Fish Project Completion Report, No. AFC-16 and AFC-25, Alaska Dept. Fish and Game.
- Drew, A. W. 1980. Initial results from a portable Dual-Beam sounder for in situ measurements of target strength of fish. IEEE Oceans 80, Int. Conf. on Eng. in the Ocean Environment.
- Ehrenberg, J. E. and T. J. Carlson, et al. 1981. Indirect measurements of the mean acoustic backscattering cross section of fish. J. Acoustic Soc. Am. Vol. 69, No. 4.
- Forbes, S. T. and O. Nakken. 1972. Manual of Methods for Fisheries Resource Survey and Appraisal. Part 2: The use of acoustic instruments for fish detection and abundance estimation. FAO Manuals in Fisheries Science, No. 5.
- Freund, J. E. 1962. Mathematical Statistics. Prentice Hall, Englewood Cliffs, N.J.

- Gradshteyn, I. S. and I. M. Ryshik. 1980. Table of Integrals, Series and Products. Academic Press, New York, N.Y.
- Huang, K. and C. S. Clay. 1980. Backscattering cross sections of live fish: PDF and aspect. J. Acoustic Soc. Am. Vol. 67, No. 3.
- Menin, A. and Paulis. 1974. Fish counting by acoustic means. IEEE Oceans 74, Int. Conf. on Eng. in the Ocean Environment.
- Nakken, O. and K. Olsen. 1977. Target strength measurements of fish. Rapp. P.-v. Reün. Cons. int. Explor. Mer. Vol. 170, Ferrier 1977.

APPENDIX A

RECEIVER -E-27  
 FREQUENCY 420 KHz  
 DATE 1-15-81 OP. \_\_\_\_\_



GATE \_\_\_\_\_  
 FILTER \_\_\_\_\_  
 XMTR IMPEDANCE: \_\_\_\_\_

SCALE: 1 dB/Div  
 PLANE \_\_\_\_\_  
 DEPTH \_\_\_\_\_  
 TEMP. \_\_\_\_\_

TRANSMITTING SENSITIVITY,  $T_v$ : 40 -G 212.5 +R 0 -V +10 -162.5 dB $\mu$ Po/V, 1 m  
 TRANSMITTING POWER RESPONSE,  $T_w$ : \_\_\_\_\_ +Z \_\_\_\_\_ dB $\mu$ Po/Watt, 1 m  
 EFFICIENCY:  $T_w$  \_\_\_\_\_ -D \_\_\_\_\_ -170.6 dB \_\_\_\_\_ %

Beam pattern of transducer used for acoustic measurements. Half angle is  $9^\circ$ .

## APPENDIX B

The tape saturation was the result of limited dynamic range of the cassette recorder, previously estimated as approximately 30 dB. Considerable effort was made towards matching or windowing the recorder dynamic range to expected dynamic range of the fish signals by adjusting system gain. However, for reasons unknown, the matching did not accommodate higher signal levels (greater than -25 dB) introducing considerable bias into the side aspect tape data.

Side aspect target strength data were recovered from the polar plots by the following method. A  $10^\circ$  sector of maximum target strength for each fish was determined from their respective polar plots. A pair of independent samples, each 125 values (25 values/degree), was obtained for each fish by examining high quality transparencies of the polar plots which were placed on an overhead projector for enlargement.

To evaluate the consistency of this sampling method, two-way Kolmogorov-Smirnov and two-sample t-tests were performed on each pair of samples. Results are in Table B1.

Table B1. Test for consistency summeries.

Fish	Maximum sector	Target strength $\bar{x}_1$	Target strength $\bar{x}_2$ (dB)	t-statistic <sup>1</sup>	K-S value <sup>2</sup>	Two-tailed P
6	261-270	-23.97	-23.94	.0150	.190	1.0
5	91-100	-23.63	-23.56	.1233	.126	1.0
4	261-270	-24.60	-24.72	.1950	.278	1.0
3	261-270	-25.78	-26.11	.5007	.389	.998
2	267-277	-24.80	-25.37	.8789	.519	.951
1	85-94	-26.53	-26.67	.2309	.326	1.0

<sup>1</sup>  $t_{0.05}(2)$ , 250 = 1.969

<sup>2</sup>  $H_0$ : The two groups are from populations with the same distribution.

$H_1$ : The two groups come from different distributions.

## APPENDIX C

## DERIVATION OF TARGET STRENGTH PROBABILITY

## DENSITY AND DISTRIBUTION FUNCTIONS

Recall the target strength (TS) definition

$$TS = 10 \log \frac{\delta_{bs}}{4\pi}$$

$$\text{Let } Z = \sqrt{\delta_{bs}}$$

$$\text{therefore } TS = 20 \log Z + k_1 \quad (C1)$$

$$\text{where } k_1 = -10 \log 4\pi$$

Equivalently one can use equation (2), therefore  $k_1 = -20 \log V_{ref} + TS_{ref}$

where  $V_{ref}$  = received voltage from reference

$TS_{ref}$  = reference target strength (known).

It is important to note in the following discussion that the random variable  $Z$  can either denote  $\sqrt{\delta_{bs}}$  or peak detected echo voltage, as long as appropriate  $k_1$  constant is used.

$$\text{Let } k_2 = 20 \log e$$

$t$  = an argument of the random variable  $TS$ ,

then the inverse function of C1 is

$$Z = g^{-1}(t) = e^{\frac{t-k_1}{k_2}}$$

Target strength is a transformation of the variable  $Z$ ; the target strength probability density function is determined by

$$f_{TS}(t) = f_Z [g^{-1}(t)] \frac{dz}{dt} \quad (\text{Freund 1962})$$

where  $f_Z$  is the Rayleigh probability density function.

Using the following substitutions,

$$C_1 = \left\{ e^{\frac{-k_1}{k_2}} \right\}^2 \frac{1}{k_2}$$

$$C_2 = \left\{ e^{\frac{-k_1}{k_2}} \right\}^2 \frac{1}{2}$$

the target strength probability density function is

$$f_{TS}(t) = \frac{e^{\frac{2t}{k_2}}}{a} \cdot C_1 \cdot \exp \left\{ \frac{-C_2}{a} e^{\frac{2t}{k_2}} \right\} \quad (C2)$$

where  $a$  = the single Rayleigh parameter.

To get the target strength probability distribution, the above density function is integrated over all possible TS values.

$$F_{TS}(t) = \frac{C_1}{a} \int_{-\infty}^{TS} e^{\frac{2t}{k_2}} \exp \left\{ \frac{-C_2}{a} e^{\frac{2t}{k_2}} \right\} dt \quad (C3)$$

$$\text{let } y = e^{\frac{2t}{k_2}}$$

$$\text{therefore } t = \frac{k_2}{2} \ln y$$

$$dt = \frac{k_2}{2} \frac{1}{y} dy$$

The integral in C3 becomes

$$\frac{k_2}{2} \frac{C_1}{a} \int_0^y e^{-\frac{C_2}{a} y} dy \quad (C4)$$

which can be evaluated, and equals

$$F(y) = 1 - e^{-\frac{C_2}{a} y} .$$

Since  $y = e^{\frac{2t}{k_2}}$ , the probability distribution function for target strength becomes

$$F_{TS}(t) = 1 - \exp \left\{ -\frac{C_2}{a} e^{\frac{2t}{k_2}} \right\} .$$

## APPENDIX D

## DERIVATION OF EXPRESSIONS FOR TARGET STRENGTH

## EXPECTED VALUE AND VARIANCE

The expected value of target strength (E [TS]) follows from the integration

$$E [TS] = \int_{-\infty}^{\infty} t \cdot f_T(t) dt$$

where  $f_T(t)$  is the target strength density function, equation (5). However, a more mathematically tractable solution follows from the relation

$$E [TS] = E [g(z)] = \int_0^{\infty} (10 \log \frac{z^2}{4\pi}) \frac{z}{a} e^{-\frac{z^2}{2a}} dz$$

where  $g(z) = 10 \log \frac{z^2}{4\pi}$  .

Simplifying the above,

$$E [TS] = \frac{20}{2.3026a} \int_0^{\infty} (\ln z) z e^{-\frac{z^2}{2a}} dz + k_1 \quad . \quad (D1)$$

To solve the integral,

$$I = \int_0^{\infty} (\ln z) z e^{-\frac{z^2}{2a}} dz$$

let  $y = \frac{z^2}{2a}$

$$z = \sqrt{2ay}$$

$$dz = \frac{\sqrt{2a}}{2} \cdot y^{-\frac{1}{2}} dy$$

$$\text{therefore, } I = a \int_0^{\infty} (\ln(2a))^{\frac{1}{2}} e^{-y} + \ln(y)^{\frac{1}{2}} e^{-y} dy$$

Completing the integral,

$$I = \frac{a}{2} [\ln 2 + \ln a - C_E]$$

where  $C_E$  is Euler's constant (.577215)

$$\text{and, } C_E = - \int_0^{\infty} e^{-x} \ln x dx .$$

Completing D1,

$$E [TS] = 4.3429 \ln(a) + .5033 + k_1 .$$

If  $4\pi$  is the reference area,  $k_1 = -10 \log 4\pi$  and

$$E [TS] = 4.3429 \ln(a) - 10.4888$$

The variance of target strength follows from the solution of the second moment

$$E_{TS} [t^2] = \int_{-\infty}^{\infty} (t^2) \frac{e^{-\frac{2t}{k_2}}}{a} \exp \left\{ \frac{-C_2}{a} e^{\frac{2t}{k_2}} \right\} C_1 dt .$$

To solve the integral,

$$I = \int_{-\infty}^{\infty} (t^2) e^{\frac{2t}{k_2}} \exp \left\{ \frac{-C_2}{a} e^{\frac{2t}{k_2}} \right\} dt$$

$$\text{let } y = e^{\frac{2t}{k_2}}$$

$$t = \frac{k_2}{2} \ln y$$

$$dt = \frac{k_2}{2} \frac{1}{y} dy$$

therefore,

$$I = \frac{(k_2)^3}{8} \int_0^{\infty} (\ln y)^2 e^{-\frac{C_2}{a} y} dy \quad .$$

From Gradshteyn and Ryzhik (1980):

$$\int_0^{\infty} e^{-\mu x} (\ln x)^2 dx = \frac{1}{\mu} \left[ \frac{\pi^2}{6} + (C_E + \ln \mu)^2 \right]$$

therefore,

$$I = \frac{(k_2)^3}{8} \frac{a}{C_2} \left[ \frac{\pi^2}{6} + \left( C_E + \ln \left( \frac{C_2}{a} \right) \right)^2 \right]$$

and

$$E_{\text{TS}} [t^2] = \frac{(k_2)^3}{8} \frac{C_1}{C_2} \left[ \frac{\pi^2}{6} + (C_E + \ln \left( \frac{C_2}{a} \right))^2 \right]$$

where, as before,  $k_2 = 20 \log e \quad (8.6859)$

$$C_1 = 1.4468$$

$$C_2 = 6.2832$$

Finally, target strength variance is found by the relation

$$\text{Var}_{\text{TS}} [t] = E_{\text{TS}} [t^2] - (E_{\text{TS}} [t])^2$$